



MISKOLCI
EGYETEM
UNIVERSITY OF MISKOLC

An atomistic view of polyurethane chemistry – A combined theoretical and experimental study

Ph.D. Dissertation

Prepared by:

Wafaa Cheikh

Supervisor:

Prof. Dr. Béla Viskolcz

Antal Kerpely Doctoral School of
Materials Science & Technology
At the Faculty of Materials Science & Engineering

Institute of Chemistry
University of Miskolc

Miskolc, Hungary
2021

“Behold! In the creation of the heavens and the earth and the alternation of the night and the day are signs indeed for those endowed of understanding.”

Quran [3:190]

Acknowledgment

First and foremost, praise and thank **God**, the Almighty, for His showers of blessings throughout my research work to complete my dissertation successfully.

I would like to express my deep and sincere gratitude to my supervisor **Prof. Dr. Béla Viskolcz** for giving me the opportunity to do research and providing invaluable guidance throughout this research.

I would like to extend my sincere and heartfelt obligation towards all members of the Institute of Chemistry and the Faculty of Materials Science and Engineering for their help, cooperation, and encouragement. A special thanks to **Dr. Béla Fiser**, **Dr. Milán Szőri**, **Dr. Zsolt Fejes**, and **Dr. Michael Owen** for conscientious guidance and encouragement to accomplish this assignment.

I also acknowledge with a deep sense of reverence, my gratitude towards **My Parents** for their love, prayers, caring, and sacrifices for educating and preparing me for the future, I hope to be always a pride for you. I am very much thankful also to my sisters and brother **Amel**, **Mohamed**, **Leila**, sister in law **Fatiha**, brother in law **Abdelkader**, and my nieces and nephew **Ines**, **Anes**, **Lilia**, and **Anya**, who has always supported me morally and encourage me.

At last but not least, gratitude goes to all of my friends who directly or indirectly helped me: **Sabah**, **Hanene**, **Ikram**, **Amina**, **Bochra**, **Edina**, **Yacine**, **Marouane**. Special thanks go to **Rabab Benotsmane**, my lovely sister in Hungary for the keen interest shown to complete this thesis successfully.

I dedicate the fruits of this work to my grandmothers, and my Prof. Dr. R.Kessas, who I lost in 2020, and with all my love; May they rest in peace.

This research was supported by the European Union and the Hungarian State, co-financed by the European Regional Development Fund in the framework of the GINOP-2.3.4-15-2016-00004 project, aimed to promote the cooperation between the higher education and the industry.

The GITDA (Governmental Information-Technology Development Agency, Hungary) is gratefully acknowledged for allocating computing resources used in this work.

Contents

List of figures.....	6
List of tables	9
List of abbreviations	10
1. Introduction	12
1.1 Synthesis process	12
1.1.1 Preparation of the prepolymer (1 st step).....	13
1.1.2 Extension of prepolymer chains (2 nd step)	14
1.2 The basic chemistry of polyurethane foams	15
1.3 Foam formulation components	16
1.3.1 Diisocyanates	17
1.3.2 Polyols.....	24
1.3.3 Water.....	25
1.3.4 Catalysts	26
2. Aims	31
3. Materials and Methods	32
3.1 Materials	32
3.2 Experimental methods	32
3.2.1 Kinetic and reactivity measurement of single urethane bond formation	32
3.2.2 Synthesis of polyurethane and mechanical properties analysis	33
3.3 Theoretical methods	36

3.3.1 Quantum Chemical Methods	37
3.3.2 Basis set	40
3.3.3 Solvation models.....	41
3.4 Applied computational methods	41
4. Results and Discussion.....	43
4.1 Urethane Formation at Isocyanate and Alcohol Excess	43
4.1.1 Experimental results on kinetic of urethane bond formation.....	44
4.1.2 Reaction mechanisms based on theoretical calculations	46
4.2 Polyurethane bond formation	52
3.2.1 Effect of mono-alcohols on polyurethane bond formation	54
5. Summary	60
6. Thesis point	62
7. Scientific publications	64
8. References	65

List of figures

Figure 1: Schematic structure of a polyurethane.....	12
Figure 2: Polyurethane synthesis of polyols and diisocyanate.....	12
Figure 3: Schematic representation of prepolymer preparation.	13
Figure 4: Copolymerization reaction.	14
Figure 5: Variation of the stress as a function of the compression deformation of a solid polymer and a foam.....	15
Figure 6: 2D structure of 4,4-diphenylmethane diisocyanate.	18
Figure 7: 2D structures of isomeric forms of TDI.	19
Figure 8: Chemical structures of aliphatic isocyanates: tetramethylxylene diisocyanate (TMXDI), isophorone diisocyanate (IPDI), and 4,4-diisocyanatodicyclohexylmethan (H12MDI).....	19
Figure 9: Mesomeric forms of the isocyanate group, where either N or O carry a negative charge.	20
Figure 10: Production of isocyanate from a primary amine via phosgenation.	20
Figure 11: First step of the “blow” reaction of water and an isocyanate. [34]	20
Figure 12: Second step of the “blow” reaction: isocyanate and amine. [34]	21
Figure 13: Formation of a biuret linkage [34].....	21
Figure 14: The gelation or cross-linking reaction of isocyanate with alcohol [34].	21
Figure 15: Allophanate formation when an isocyanate and urethane react [34].....	22
Figure 16: The reaction of an isocyanate with a nucleophilic agent.	22
Figure 17: The spontaneous formation of uretidione from two aromatic isocyanates at 25 °C.	23
Figure 18: The carbodiimide formation from two isocyanates between 150 °C and 300 °C.	23
Figure 19: The polycarbodiimide formation from carbodiimide functional group.....	24

Figure 20: The formation of a substituted uretonimine from carbodiimide and isocyanate...	24
Figure 21: The isocyanurates formation of three high reactive isocyanates.	24
Figure 22: The polyamide-1 formation between -100 °C to -20 °C.	24
Figure 23: Schematic structure of polyether polyols.	25
Figure 24: Chemical structure of water.....	26
Figure 25: Schematic structure of a tertiary amine.	26
Figure 26: Activation of an alcohol by an amine during urethane formation.	27
Figure 27: Activation of isocyanate by an amine during urethane formation.....	28
Figure 28: Chemical structure of polydimethylsiloxane.....	28
Figure 29: Chemical structure of diethanolamine.....	29
Figure 30: Chemical structure of hydroquinone.	30
Figure 31: Microreactor setup. The Asia microflow system (Syrris Ltd., Royston, UK).....	33
Figure 32: Compressive test of foam specimen with the Instron® 5566 universal testing machine.	36
Figure 33: Reaction mechanism for urethane bond formation. Alcohol excess mechanism (top) involves hydrogen-bonded alcohol associate as reactant while isocyanate excess mechanism (bottom) starts with dipole-dipole stabilized intermolecular isocyanate dimer. In the present study R = Propane and Ar = Phenyl.....	43
Figure 34: Experimental kinetic curves. (a) Second-order kinetics for the stoichiometric ratio (b) pseudo-first-order kinetics for the 20-fold PhNCO excess. Data points used for fitting and reaction rate constants determination are indicated by solid curve segments.....	44
Figure 35: Arrhenius plot.....	45
Figure 36: Energy profile (zero-point corrected) for the alcoholic route in 1-PrOH (red solid line), and in THF (red dashed line), and for the isocyanate route in 1-PrOH (blue solid line),	

and in THF (blue dashed line) calculated by using the G4MP2 composite method in combination with the SMD implicit solvent model.	47
Figure 37: Reactive complex (RC), transition state structure (TS) and product complex (PC) structures (obtained at B3LYP/6-31G(2df,p) level of theory from G4MP2 calculation) for the excess alcohol reaction mechanism of urethane bond formation in solvent 1-PrOH or THF (in parenthesis). The relative zero-point corrected energies are also presented in $\text{kJ}\cdot\text{mol}^{-1}$	48
Figure 38: Reactive complex (RC), transition state structure (TS), intermediate (IM) and product complex (PC) structures (obtained at B3LYP/6 31G(2df,p) level of theory from G4MP2 calculation) for the isocyanate excess reaction mechanism of urethane bond formation in solvent 1-PrOH or THF (in parenthesis). The relative zero-point corrected energies are also presented in $\text{kJ}\cdot\text{mol}^{-1}$	50
Figure 39: Polyurethane synthesis modified by a monoalcohol ($\text{R}_3\text{-OH}$).....	53
Figure 40: Flexible polyurethane foams, all with the concentration of mono-alcohols at the range of 0.2, 0.5, 1.0, and 2.0%	54
Figure 41: Height of flexible polyurethane foams with methanol and ethanol at concentrations of 0.2, 0.5, 1.0, 2.0%.	55
Figure 42: Densities of polyurethane foams as a function of monoalcohol concentration.	55
Figure 43: Densities of polyurethane foams as a function of monoalcohol concentration.	56
Figure 44: The Plot of Young's modulus vs density.	58
Figure 45: A chart of Young's modulus and density for materials created using the CES EduPack 2007 software with the Level 2 database.	59

List of tables

Table 1: Typical components and their normal usage in flexible polyurethane foam formulations [21].....	17
Table 2: The most frequently used commercial amino compounds in the production of polyurethane.	27
Table 3: Experimental reaction rate constants (k_A , k_S , and k_I) at different temperatures, Arrhenius activation energies (E_a), and pre-exponential factors (A). E_a and A values were obtained by the method of least squares. For $[NCO]_0 / [OH]_0 = 0.005$, data are taken from [121]. (<i>n.m.</i> = <i>not measured</i>)	45
Table 4: G4MP2 thermochemical properties calculated in 1-propanol (PrOH) and tetrahydrofuran (THF) including zero-point corrected relative energies (ΔE_0), relative enthalpies ($\Delta H(T)$) and relative Gibbs free energies ($\Delta G(T,P)$) at $T = 298.15$ K, and $P = 1$ atm, A in excess alcohol, and I in excess isocyanate. All values are in $\text{kJ}\cdot\text{mol}^{-1}$	46
Table 5: Relative enthalpies of all the transition state of the reaction at excess alcohol and excess isocyanate, obtained with different methods of calculation ($\Delta H(T)$) at $T = 298.15$ K, and $P = 1$ atm, calculated in 1-propanol (PrOH) comparing to the experimental Arrhenius activation energies (E_a) and calculated (E_a^{G4MP2}), ATS according to alcohol excess, and ITS1 to isocyanate excess. All values are in $\text{kJ}\cdot\text{mol}^{-1}$	51
Table 6: The components and the typical concentration used in the production of modified flexible polyurethane foam.....	53
Table 7: Density and mechanical properties of polyurethane flexible foams.	57

List of abbreviations

PU	Polyurethane
MDI	Methylene diphenyl diisocyanate
MDA	Methylene diphenyl diamine
TDI	Toluene diisocyanate
DMCHA	N,N-Dimethylcyclohexylamine
PhNCO	Phenyl isocyanate
PrOH	1-Propanol
THF	Tetrahydrofuran
ACN	Acetonitrile
HPLC	High-performance liquid chromatography
PES	Potential energy surface
TS	Transition state
IM	Intermediates
IRC	Intrinsic reaction coordinate
MEP	Minimal energy pathways
DFT	Density functional theory
MO	Molecular orbital
QM	Quantum mechanical
HF	Hartree-Fock
BO	Born-Oppenheimer approximation
MP	Moller-Plesset perturbation
CC	Coupled-cluster
QCISD(T)	Quadratic Configuration Interaction with Single and Double substitutions
B3LYP	Becke, 3-parameter, Lee-Yang-Parr
HLC	Higher-level correction
CBS	Complete basis set
pVDZ	Double zeta basis set
pVTZ	Triple zeta basis set
SMD	Solvation model based on density
k_s	Rate constants for the stoichiometric reaction
k_A	Rate constants for the reaction in excess alcohol

k_I	Rate constants for the reaction in excess isocyanate
E_a	Arrhenius activation energy
ΔE_0	Zero-point corrected relative energy
$\Delta H(T)$	Relative enthalpy
$\Delta G(T,P)$	Relative Gibbs free energy
ΔfH°	Heat of formation
$\Delta H^\circ_{\text{vap}}$	Enthalpy of vaporization
A_RC	Reactive complex of the reaction in excess alcohol
ATS	Transition state of reaction in excess of alcohol
A_PC	Product complex of reaction in excess of alcohol
I_RC	Reactive complex of the reaction in excess isocyanate
ITS1	First transition state of the reaction in excess isocyanate
I_IM	Intermediate of the reaction in excess isocyanate
ITS2	Second transition state of the reaction in excess isocyanate
I_PC	Product complex of the reaction in excess isocyanate
pbw	Parts by weight
E	Young's modulus
ρ	Density

depends on the structure of both the alcohol and isocyanate. [4][5] Certain industrial processes which are used to produce polyurethane elastomers, use a single step ("one-shot" process) polyaddition, and thus, this process is easier, faster, and more reproducible. This is particularly the case with foam manufacturing.

However, the process of using a prepolymer involves two steps. In the first step, the isocyanate prepolymer is prepared by the reaction between diisocyanate in slight excess and a polyol. In the second step, the isocyanate prepolymer is placed in the presence of a polyfunctional polyol (chain extending or a hydroxylated crosslinking agent of low molar mass) leading to the formation of the final polymer. The temperature of the reaction of this last step is between 80 °C and 110 °C. [6] The use of a prepolymer makes it possible to modulate the reactivity, viscosity, functionality, the amount of free isocyanates, or even the volatility of the isocyanates. This makes it possible to overcome the problem that can arise from the difference in reactivity between macrodiol and chain extender, which enables more control of the properties of the polymer and also makes it possible to yield compounds that are less toxic than the diisocyanate starting material.

The 2-step process is detailed by Oertel [7] as follows:

1.1.1 Preparation of the prepolymer (1st step)

Polyaddition reaction between an alcohol and an isocyanate (**Figure 3**).

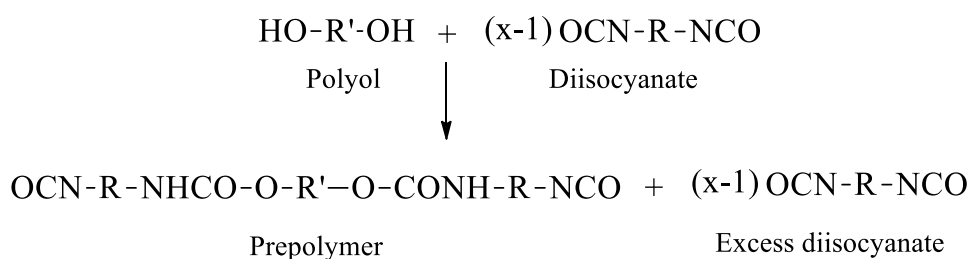


Figure 3: Schematic representation of prepolymer preparation.

The isocyanate functional groups and the active hydrogens of the polyol result in the formation of urethane bonds. These urethane bonds are at the heart of a prepolymer. The prepolymer is therefore a mixture of polyol chains more or less elongated by diisocyanate molecules via urethane bonds, and excess diisocyanate.

The prepolymer is characterized by its NCO number which corresponds to the number of grams of NCO groups present in 100 grams of diisocyanate prepolymer.

1.1.2 Extension of prepolymer chains (2nd step)

This stage is known as the copolymerization phase which allows the transition from the reactive mixture to the final polymer (**Figure 4**).

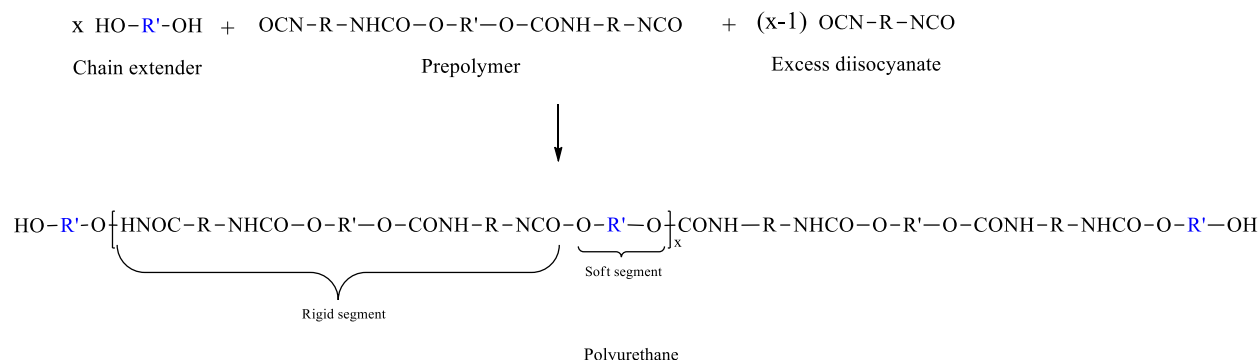


Figure 4: Copolymerization reaction.

The resulting polyurethanes consist of blocks of flexible chains with a low glass transition temperature (called flexible segments) originating essentially from macrodiol and of highly polar, relatively rigid blocks (called rigid segments). The flexible segments are generally polyesters or polyethers. The rigid segments are formed by the reaction of the diisocyanate with the chain extender. As for the final materials, the length of the rigid segments, which is linked to the amount of free diisocyanate, and the chain length of the prepolymer also directly influence the molar mass between physical crosslinking nodes formed by the rigid domains and therefore the elasticity of the final material. [8]

In addition to the isocyanate, the polyol is the other essential component for the formation of polyurethanes. [9][10]

The formation of the polyurethane backbone results from the reaction between an isocyanate prepolymer and a polyol of comparable mass. In the case where the isocyanate prepolymer is bifunctional, the use of a macrodiol will lead to the formation of a linear polyurethane. If the functionality of the polyol, which refers to the number of OH groups per molecule, is greater than two, the polyurethane formed will be a three-dimensional network.

Starting from two bifunctional alcohols and isocyanate prepolymers, it is possible to obtain a three-dimensional network by using low molecular weight polyfunctional alcohols. Glycerol is an example of such alcohol, which can act as a crosslinking agent.

Low molecular weight diols such as 1,4-butanediol are also used to control the kinetics of polyurethane formation. These alcohols are called chain extenders.

1.2 The basic chemistry of polyurethane foams

There are two main important reactions in the production of flexible polyurethane foams.

The blow reaction and the gelation reaction. For the manufacture of flexible foams, the balance between the respective rates of these two reactions creates the open cell morphology of the foam, which is very important for its physical properties.

Polymer foams consist of a distribution of gas trapped in a solid matrix. Due to their lightness, sound and heat insulation, and impact resistance they are used in the transportation industry as well as in furniture or buildings. The first main characteristic of a foam is its low density. The accessible density range is from 1.6 to 960 kg·m⁻³ for polystyrene and from 10 to 800 kg·m⁻³ for polyurethane [11]. This lightness is essential for aeronautical applications. Its second main characteristic is its ability to undergo large compression deformations for a relatively low level of stress [12]. In **Figure 5**, we qualitatively compare the compression behavior of a solid polymer to that of foam. If we can consider that the stress is a quasi-linear function of the deformation for a polymer, in the case of foam, a plateau appears. This corresponds to the crushing of the cells of foams, i.e. the compaction phase. As the magnitude of the stress further increases, the deformation behavior is similar to that of the solid polymer. During deformation, a large amount of energy is absorbed by the foam, which is why these materials are used as shock absorbers in the automotive industry. This behavior is strongly influenced by the cellular structure of the foam. [13]

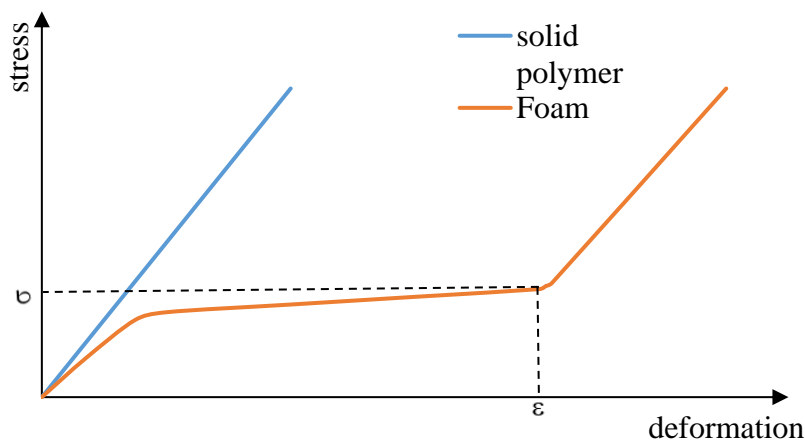


Figure 5: Variation of the stress as a function of the compression deformation of a solid polymer and a foam.

Between rigid and flexible foams, a distinction is made according to the mechanical properties of the matrix. The matrix is either made of a thermoplastic polymer such as polystyrene, or a

thermoset polymer such as polyurethane. In the first case, the production of the foam is independent of the synthesis of the polymer. For thermosets, the production of foam is simultaneous with the synthesis of the polymer.[14]

The cells present in the foams are either open or closed. To achieve the structure of the cells a blowing agent should be used which can be:

- physical: a gas is injected under pressure to allow its solubilization in the polymer liquid.
- chemical: a compound which reacts during the polymer matrix formation and this reaction leads to a gaseous side product.

The most widely used physical blowing agents were chlorofluorocarbons or CFCs. However, the use of these molecules has been banned because of their involvement in the destruction of the ozone layer, as outlined in the Montreal Protocol. [15] Since the early 1990s, they have mostly been replaced by hydrofluorocarbons or HFCs which do not pose any danger to the ozone layer. Unfortunately, these compounds are greenhouse gases which is stated in the Kyoto Protocol. [16] Currently, polymer foams are produced with carbon dioxide under supercritical conditions. [17][18][19][20]

Water is the most common chemical blowing agent used to produce polyurethane foams, which reacts with the isocyanate and generates carbon dioxide. Water will be used in our study as the principal blowing agent.

The formation of a polyurethane foam involves two concomitant reactions: the polymerization reaction and the expansion reaction. To obtain a suitable foam, the time necessary for the formation of the network must be similar to the time necessary for the expansion of the foam. If this condition is met, the structure of the foam will be regular and it will be possible to obtain a material with a very low density ($<50 \text{ kg}\cdot\text{m}^{-3}$) offering very good insulating and damping properties. The density will also define the rigidity of the desired foam (rigid, semi-rigid, high or low density).

1.3 Foam formulation components

Each application of flexible polyurethane foams has specific performance criteria, thus many components are needed to ensure that the product of a typical formulation will be open-cell and still meet other requirements too. For example, fillers may be added to enhance strength, or a lower potency surfactant may be used to increase cell openness. An example of the types of

components that might be involved in a formulation, and some exemplary concentration ranges are provided in **Table 1**. It should be noted that, by convention, flexible polyurethane foam formulations are calculated as weight fractions based on total polyol added (parts per hundred polyol). The type of each component will be discussed in detail in the following subsections.

Table 1: Typical components and their normal usage in flexible polyurethane foam formulations [21]

Component	Weight Added [Parts Per Hundred Polyol]
Polyol	100
Water	1.5-7.5
Inorganic fillers	0-150
Silicone surfactant	0.5-2.5
Amine catalyst	0.1-1.0
Tin catalyst	0.0-0.5
Chain extender	0-10
Crosslinker	0-5
Auxiliary blowing agent	0-35
Isocyanate	25-85

1.3.1 Diisocyanates

A wide range of compounds containing at least two isocyanate functional groups is currently used in the flexible foam industry, which can be aliphatic or aromatic.

Aromatic isocyanates

The NCO functional group is directly attached to the aromatic skeleton. This enables the delocalization of the negative charges into the π electron ring system which further increases the positive charge of the carbon atom, thus making the aromatic isocyanates much more reactive than the aliphatic ones [22].

Aromatic are relatively inexpensive. However, they can generate materials that are sensitive to photolytic aging. Indeed, the possible oxidation of aromatic compounds by UV radiation can cause the change of color (yellowing) of the corresponding products. Therefore, these are used for the production of polyurethanes with specific applications of adhesives or coatings where color is not an essential aspect[23][24]. The two aromatic isocyanate types which are widely

used in the synthesis of polyurethanes are methylene diphenyl diisocyanate (MDI) and toluene diisocyanate (TDI) [25][26].

a. Methylene diphenyl diisocyanate (MDI)

Methylene diphenyl diisocyanate, is derived from the condensation reaction of aniline with formaldehyde, which forms polymeric amines that are then phosgenated. This results in a mixture of various forms of MDI, and this process will be described in more detail in a later chapter. The mechanism of the phosgenation of MDA will be investigated using accurate quantum chemical calculations, and the gas phase thermodynamic profiles of the possible reaction pathways leading to the formation of the MDI will be investigated thereafter. Where MDI is generally produced in the form of 4,4'-diphenylmethane diisocyanate (**Figure 6**), however, traces of the 2,4' and 2,2' isomers can be found[27].

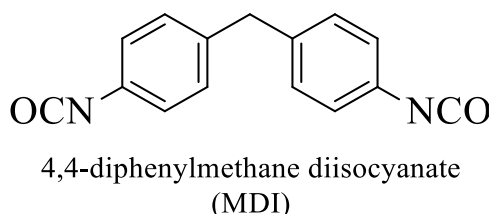


Figure 6: 2D structure of 4,4'-diphenylmethane diisocyanate.

The MDI group has a fairly rigid structure and spontaneously dimerizes at low temperatures. Although it is slow, this dimerization step alters the properties of the product. The perfect symmetry of 4,4'-MDI suggests that the two NCO functions should, in theory, have the same reactivity. In practice, kinetic studies have shown that the second NCO group is half as reactive once the first has reacted [28]. Indeed, at 25 °C, the reactivity ratio of the two functions is two, while it tends towards one beyond 100 °C [29]. This difference in reactivity is due to the resonance effect of the aromatic nuclei [30].

b. Toluene diisocyanate (TDI)

TDI exists in two isomeric forms, 2,4- and 2,6-toluene diisocyanate (**Figure 7**). TDI is synthesized from toluene. It includes a nitration step followed by a reduction step, which yields either of the two aforementioned diaminotoluene isomers. A final reaction with phosgene yields the TDI end-product.

In addition to its low resistance to ultraviolet radiation, the low vapor pressure of TDI makes it particularly toxic. Indeed, it causes breathing discomfort and irritation of the lungs[29][31]. The NCO group on carbon 4 of 2,4-toluene diisocyanate (**Figure 7**) is much more reactive than

those on carbon 2. Once the first NCO group has reacted, the second NCO is approximately 8 times less reactive than the first one [32].

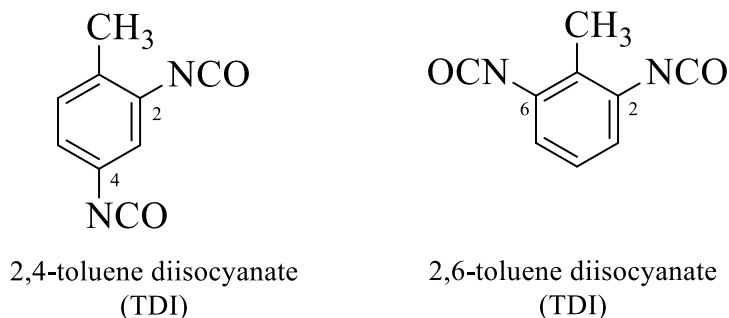


Figure 7: 2D structures of isomeric forms of TDI.

Aliphatic isocyanates

The NCO group in aliphatic isocyanates is not directly linked to a double bond, which gives polyurethanes based on these structures excellent resistance to light and aging.

The aliphatic nature of these isocyanates leads to a lower reactivity, thus these isocyanates react more slowly and require the use of a catalyst. Their reactivity with carboxyl groups and with water is also lower and there is no self-condensation reaction. These isocyanates allow the synthesis of prepolymers at temperature ranges of 100-120 °C, compared to the 60-80 °C reaction temperature used for aromatic isocyanates [30], [33]. For all these reasons, they are generally preferred to aromatic isocyanates for the formulation of polyurethane foam, despite their much higher cost. The three aliphatic isocyanates mostly used in the synthesis of polyurethanes are tetramethylxylene diisocyanate (TMXDI), isophorone diisocyanate (IPDI), and 4,4'-diisocyanatodicyclohexylmethane (H12MDI), see **(Figure 8)** [26].

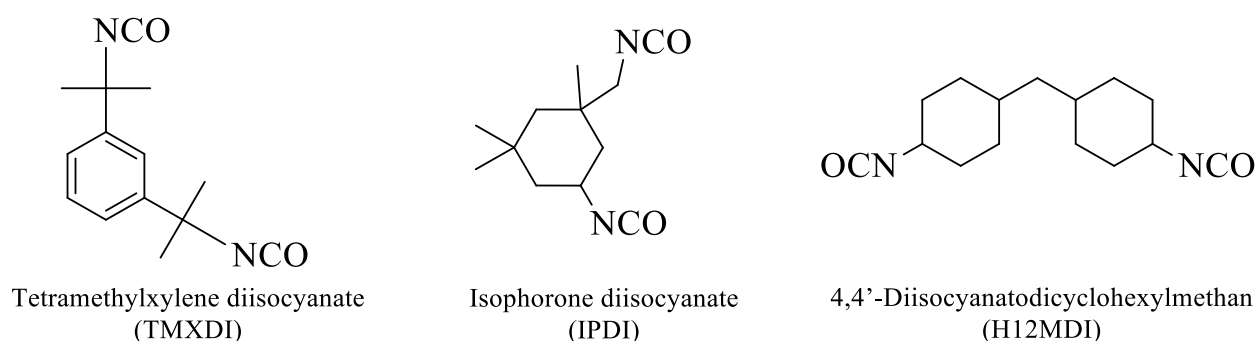


Figure 8: Chemical structures of aliphatic isocyanates: tetramethylxylene diisocyanate (TMXDI), isophorone diisocyanate (IPDI), and 4,4'-diisocyanatodicyclohexylmethane (H12MDI).

Isocyanate chemistry

The synthesis of urethanes is based on the chemistry of the isocyanate group which has two mesomeric forms (**Figure 9**).

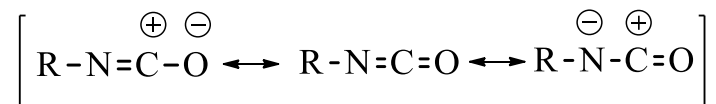


Figure 9: Mesomeric forms of the isocyanate group, where either N or O carry a negative charge.

Isocyanates are highly reactive, carry one or more N=C=O functional groups and prepared by reacting phosgene with amines (**Figure 10**) [21]. The two double bonds N=C and C=O within the isocyanate allow it to react with all compounds with active hydrogens such as alcohols or amines.

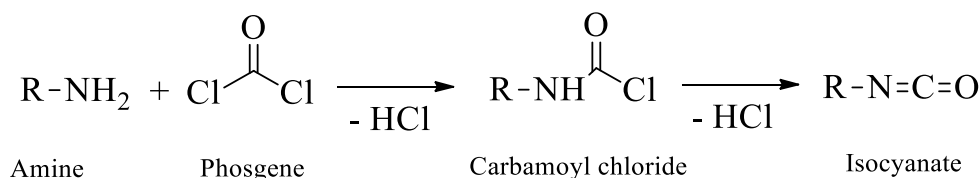


Figure 10: Production of isocyanate from a primary amine via phosgenation.

a. “Blow” reaction

The reaction of water with isocyanates is a two-step process called the “blow” reaction because, in addition to the production of polyurea, a gas is released which plays an essential role in the foaming process. Auxiliary blowing agents can also be used to give a softer foam compared to using water alone as described in **section 1.3.7**. This reaction proceeds through an intermediate where a thermally unstable carbamic acid is generated, which spontaneously decomposes to form carbon dioxide and an amine. The diffusion of carbon dioxide into the bubbles already nucleated causes the foam to expand (**Figure 11**). Besides this, the heat produced will also play an important role in the expansion of the gas in the liquid to form the desired cellular morphology. Heat generated from the “blow” reaction is 196.6 kJ·mol⁻¹. [21]

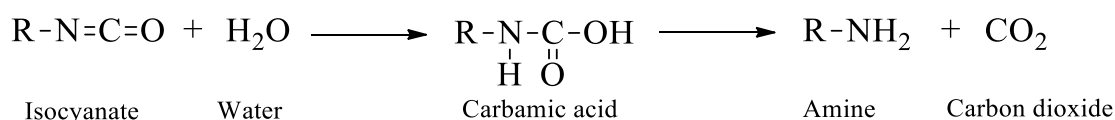


Figure 11: First step of the “blow” reaction of water and isocyanate. [34]

The second step of the reaction will occur between the formed amine and another isocyanate group and will lead to a disubstituted urea (**Figure 12**). This reaction can also be a source of covalent crosslinks if the isocyanate has more than two functional groups.

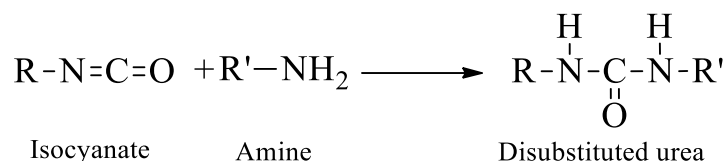


Figure 12: Second step of the blowing process: reaction of an isocyanate and an amine. [34]

The disubstituted urea which is the product of the “blow” reaction (**Figure 12**) could also react with an isocyanate group which will lead to the formation of a biuret. However, this reaction is reversible and generally does not occur below 100 °C (**Figure 13**).

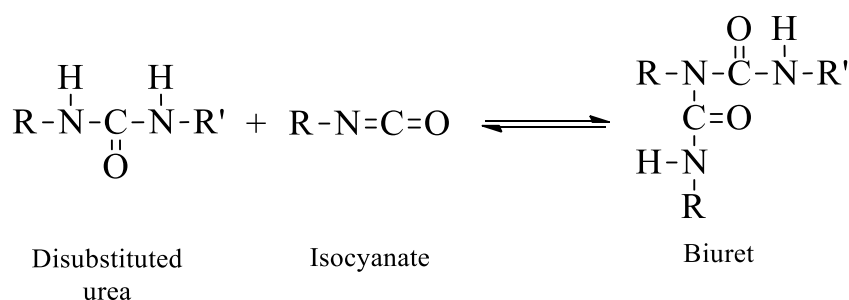


Figure 13: Formation of a biuret linkage [34].

b. Gelation reaction

Polyurethane is produced by the reaction between an alcohol and an isocyanate. This reaction is exothermic with a heat of about 100 kJ·mol⁻¹ [21] (**Figure 14**). The nature of the R groups and the R' groups can vary depending on the selection of the components of the formulation (R and R' are alkyl or aryl groups).

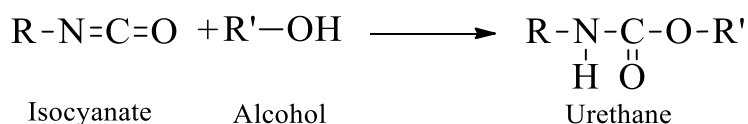


Figure 14: The gelation or cross-linking reaction of isocyanate with alcohol [34].

We have seen that isocyanates react preferentially with compounds with active hydrogen, but other reactions are also possible [35][36], such as the formation of allophanates (**Figure 15**). This occurs when another free group of isocyanate reacts with the urethane bond between 100 °C and 140 °C using the hydrogen of the carbamate group [37][38].

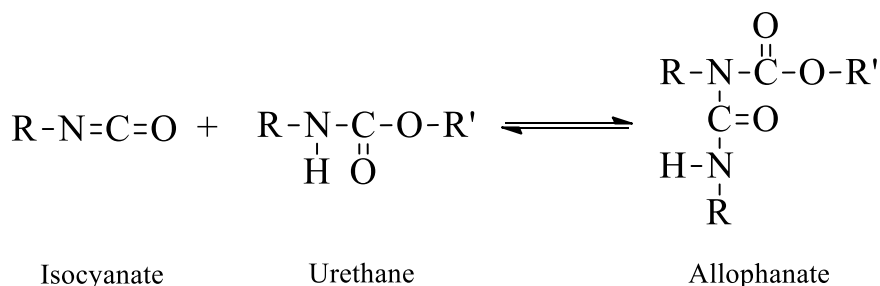


Figure 15: Allophanate formation from an isocyanate and a urethane [34].

Side reactions of isocyanates

a. Alternative route of the alcohol–isocyanate reaction

The reactivity of isocyanates comes from the strong electrophilic nature of the carbon atom, which is enhanced in the case of aromatic isocyanates. In the absence of a catalyst, the addition reaction of a proton donor to isocyanate involves the formation of an intermediate complex. The reaction begins with a nucleophilic attack on the carbon of the isocyanate and leads to the formation of two mesomeric forms. The intermediate complex formed by the addition of a second molecule R'-H decomposes according to a proton exchange reaction. Depending of which mesomer is present, the final products are not identical (**Figure 16**) [38].

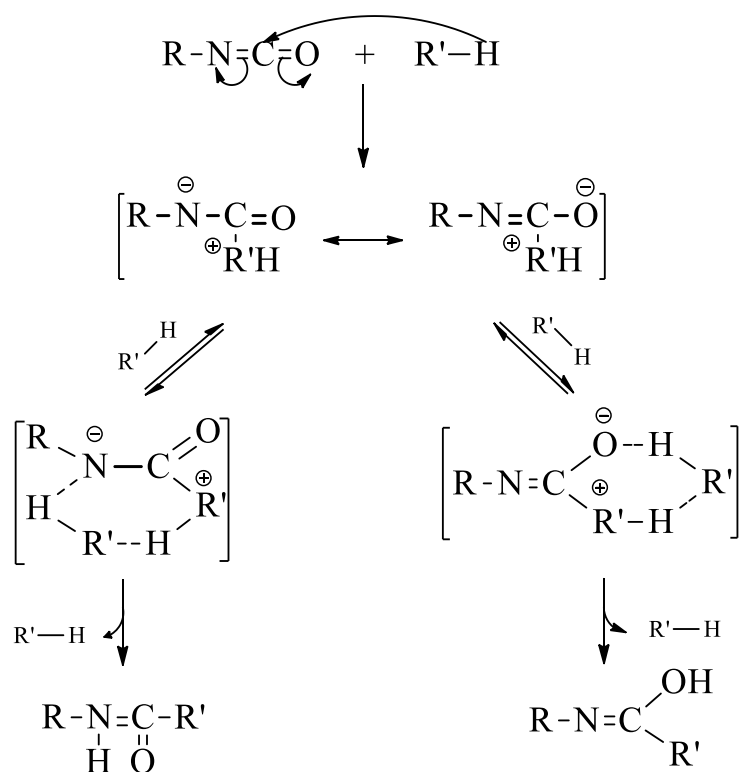


Figure 16: The reaction of an isocyanate with a nucleophilic agent.

b. Self-reactions of isocyanates

Isocyanates can also react with each other and lead to the formation of isocyanate dimers, trimers, or even polymers. Isocyanates of high reactivity are likely to dimerize. The dimerization reaction is favored by a reaction temperature between 20 °C and 80 °C in the presence of a basic catalyst such as trialkyl phosphines[39], and leads to the formation of uretidione. Aromatic isocyanates tend to form uretidiones spontaneously, even during their storage at room temperature, in the solid-state and without a catalyst (**Figure 17**). The formation of diisocyanate dimers alters the initial stoichiometry calculated for the isocyanate unless the reaction temperature is high enough to decompose the dimers. For example, the dissociation of cyclic uretidione occurs spontaneously between 150 °C and 180 °C [39].

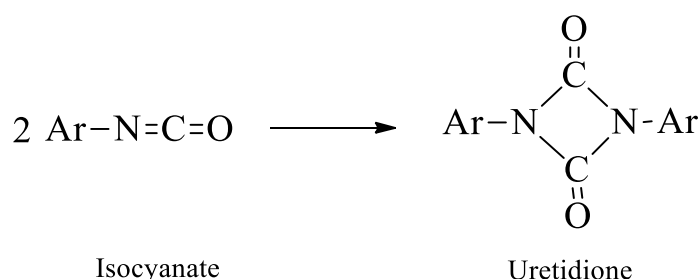


Figure 17: The spontaneous formation of uretidione from two aromatic isocyanates.

As with dimerization, isocyanates of higher reactivity are able to trimerize to form isocyanurates, which are characterized by high thermal stability. Moreover, due to the effective catalysts, their formation often occurs as a secondary reaction during synthesis. Trimerization is favored by harsh reaction conditions, such as the presence of strong bases, if the isocyanates used are very reactive. Trimerization is frequently accompanied by dimerization and the formation of a carbodiimide, between 150 °C and 300 °C, without a catalyst (**Figure 18**) [40][41].

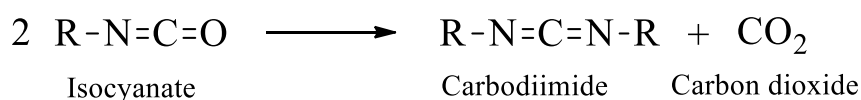


Figure 18: The carbodiimide formation from two isocyanates.

In case of diisocyanates, this reaction could yield a polycarbodiimide (**Figure 19**). Besides that, a carbodiimide functional group can react again with an isocyanate and form substituted uretonimines (**Figure 20**). Isocyanurates are formed during trimerization (**Figure 21**) [42].

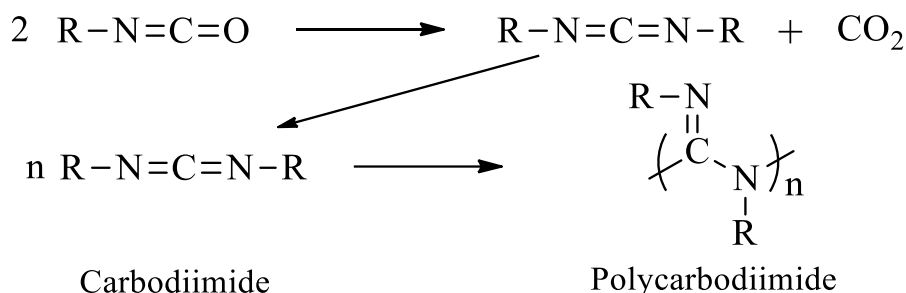


Figure 19: The polycarbodiimide formation from carbodiimide functional groups.

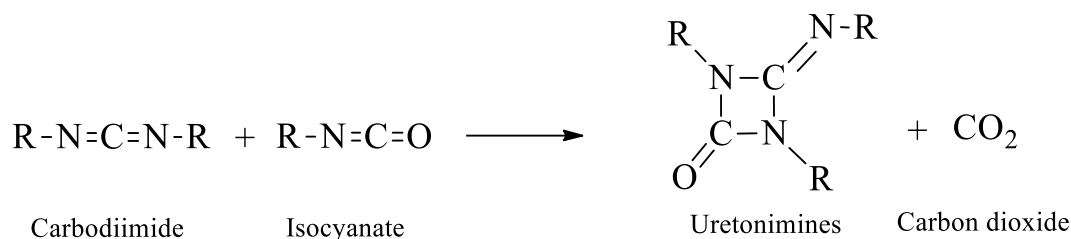


Figure 20: The formation of a substituted uretonimine from carbodiimide and isocyanate.

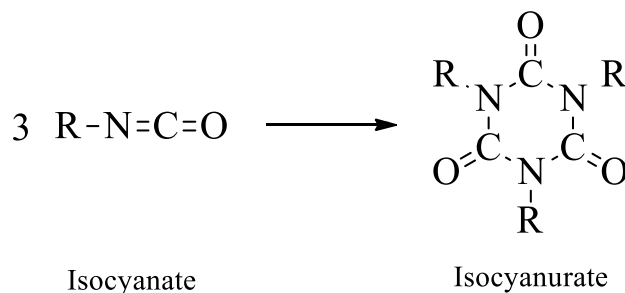


Figure 21: The isocyanurates formation from three highly reactive isocyanates.

Finally, isocyanates can undergo linear polymerization at very low temperatures (-100 °C to -20 °C for certain monoisocyanates), in the presence of anionic initiators. The final polymer obtained in this case would be polyamide-1 (**Figure 22**) [42].

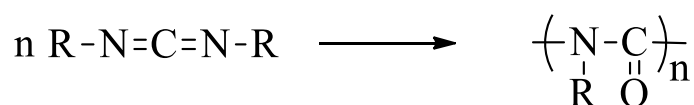


Figure 22: The polyamide-1 formation between -100 °C to -20 °C.

Studying the literature highlights, the reaction mechanisms associated with the isocyanate group are complex. Many of these mechanisms remain hypothetical and their validation would still require years of research.

1.3.2 Polyols

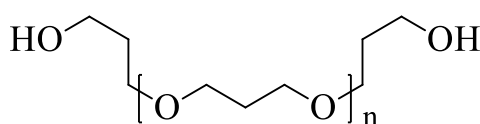
The second component of polyurethane foam formulation is the polyol, which can be any molecule containing at least two hydroxyl groups. It was mainly the use of a wide range of

polyols of different properties, molecular weights, and different functionalities that allowed the development of the very high diversity of polyurethanes. Polyols are generally an alcohol-functionalized low molecular weight polymers ($3,000$ to $5,000 \text{ g}\cdot\text{mol}^{-1}$) that can be classified into two categories, monomeric and polymeric polyols. Monomeric polyols are low molecular weight organic compounds, such as glycerol, ethylene glycol, propylene glycol, diethylene glycol, and 1,4-butanediol. Monomeric polyols are thus classified according to the number of hydroxyl groups in a molecule, such as diols, which have two hydroxyl groups in a molecule, triols which have three hydroxyl groups in a molecule, and so on [43][44].

Polymeric polyols are high molecular weight polymers obtained from ethylene oxide or propylene oxide, and are major components for the formation of polyurethane backbones. Polyether and polyester polyols are the two most common polymeric polyols [45][46]. Therefore, their specific composition is frequently tailored to meet very specific requirements, they are cheap, easy to handle, and are more resistant to hydrolysis than polyesters are [21].

Polyethers

The hydroxylated polyethers are generally obtained by the polyaddition, either anionic or cationic, of cyclic monomers such as ethylene oxide, propylene oxide, or even tetrahydrofuran. The molar masses of the polyether polyols used in the synthesis of polyurethanes vary from 250 to $8000 \text{ g}\cdot\text{mol}^{-1}$. Their functionality can range from 2 to 7 groups depending on the nature of the molecule used as an initiator. The terminal groups of these polyether diols can be either primary or secondary alcohols (**Figure 23**).



Polyether polyols

Figure 23: Schematic structure of polyether polyols.

However, the main advantage of this family of polyols is their cost, which is particularly low, because of the high availability of the raw materials used in their manufacture.

1.3.3 Water

Water (**Figure 24**) is added to these formulations to react with the isocyanate as discussed in **Section 1.2**. This reaction ultimately produces polyurea, carbon dioxide, and heat [47]. This carbon dioxide diffuses to existing gas bubbles in the polyol and so expands the mixture into a

foam. Controlling the amount of air contained in the polyol raw material is one way by which manufacturers control the number of nucleation sites in the reacting mixture. These initially small bubbles quickly grow through either gaining gas from the diffusing carbon dioxide or by coalescing with other bubbles.

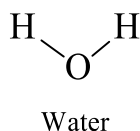


Figure 24: Chemical structure of water.

1.3.4 Catalysts

Catalysis is essential to obtain polyurethanes in an economically viable time. From an industrial point of view, the production of a foam must be accomplished in about ten minutes. The flexible polyurethane foams are the product of two competing reactions, and a good balance of these reaction rates is necessary to obtain a good open-cell morphology at the desired density. The formation of a foam involves the synthesis of the polymer network and the release of an agent that allows it to expand [48][49][33]. The catalysts most often used for the synthesis of polyurethane foam are tertiary amines or organometallic compounds [50]. Tertiary amines behave like Lewis bases and organometallic compounds behave like Lewis acids [49][33][51]. The most commonly used type of catalyst is the tertiary amines that take part in our experimental studies.

1.3.4.1 Tertiary amines

These catalysts are generally thought of as blowing catalysts but they also enhance the gelation reaction. The lone electron pair on the nitrogen atom (**Figure 25**) provides a strong nucleophile that is capable of attacking the carbon of the isocyanate group [52].

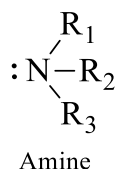
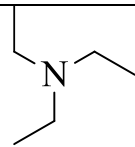
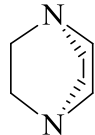
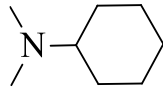
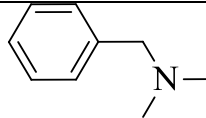
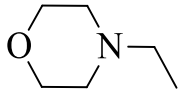


Figure 25: Schematic structure of a tertiary amine.

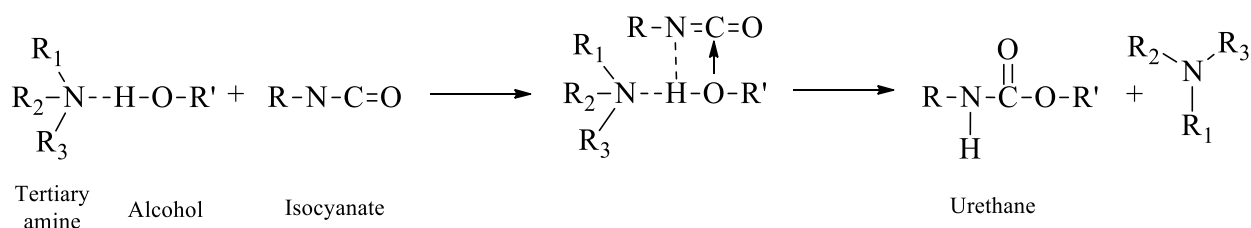
Steric hindrance and electronic effects of the substituent groups are the two main tools used to adjust the relative catalytic activity of the various tertiary amines. In some foam systems, specific combinations of amines are used to balance the rates of the gelation and blow reactions.[53][51][54].

Table 2: The most frequently used commercial amino compounds in the production of polyurethane.

Name of the amine	Abbreviation	Formula
Triethylamine	TEA	
1,4-diazabicyclo[2.2.2]octane or triethylenediamine	DABCO or TEDA	
<i>N,N</i> -dimethylcyclohexylamine	DMCHA	
Benzyltrimethylammonium chloride	BDMA	
<i>N</i> -ethylmorpholine	NEM	

There are two modes of catalysis for amines. It has been shown that when they react, they create interactions with available active hydrogens and thus activate the reagent [55].

A complex between the isocyanate and an alcohol can then be formed more easily due to the interaction between the tertiary amine and the alcohol (**Figure 26**), leading to urethane bond formation.

**Figure 26:** Activation of an alcohol by an amine during urethane formation.

The second mode of the catalysis is favoured by a strong nucleophilicity induced *inter alia* by a light steric hindrance of the amine nitrogen. This can then bind to the electropositive carbon of the isocyanate and thus activate this function by increasing the partial charge of nitrogen and oxygen [56], as shown in (**Figure 27**). The alcohol can then form a complex and can react more easily.

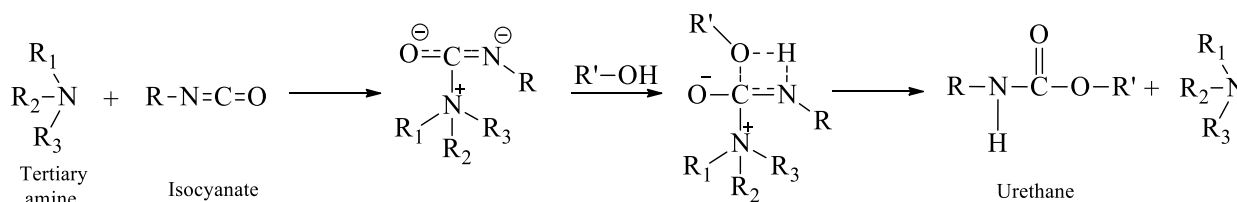


Figure 27: Activation of an isocyanate by an amine during urethane formation.

High basicity favors the isocyanate - water reaction. In addition, the increasing number of amine groups in the molecule makes it possible to increase the catalytic activity of the catalyst and to promote in particular the activation of water. In the section on the theoretical and experimental methods, we will study the association of reagents in the absence of catalysts.

1.3.5 Surfactants

Non-ionic surfactants are ubiquitous in the flexible polyurethane foam industry for the production of a good open-cell morphology. Some of the functions they perform are reducing surface tension, emulsifying incompatible ingredients, promoting bubble nucleation, stabilizing the rising foam, and reducing the defoaming effect. Of these, the most crucial to foam production is the stabilization of the cell walls. The most common surfactants in use today are graft copolymers consisting of polydimethylsiloxane (**Figure 28**) and the groups of polyethylene oxide and propylene oxide [34][21]. The mechanical properties of hard polyurethane foams such as air permeability and cell size, are greatly influenced by the structure of the silicone surfactant used in the formulation.

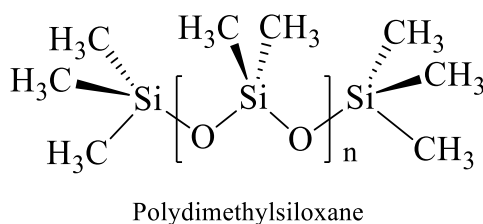


Figure 28: Chemical structure of polydimethylsiloxane.

A series of silicone surfactants with different structures have been tested in polyurethane manufacturing. Surfactants with a higher silicone content provide a lower surface tension and help increase the number of air bubbles introduced during mixing [57].

1.3.6 Cross-linking agents

In polyurethane systems, cross-linking agents are typically short-chain molecules containing amine or hydroxyl functional groups and having a functionality greater than three. They can be added to the formulation to provide increased load-bearing or initial foam stability [58]. The

most frequently used commercial cross-linking agents in polyurethane foam production are ethylene glycol, diethylene glycol, propylene glycol, dipropylene glycol, 1,4-butanediol, 1,6-hexanediol, glycerol, trimethylolpropane, and diethanolamine (**Figure 29**).

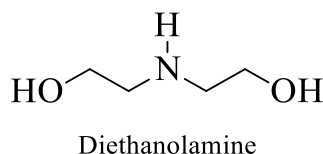


Figure 29: Chemical structure of diethanolamine.

These cross-linkers are most frequently used in molded foam formulations. The high molecular weight polyols and the faster reaction rates observed in those systems build viscosity so fast that the use of typical foam surfactants overstabilizes the cell walls, thus preventing many cells from opening. To allow cell opening to occur, lower-potency surfactants are utilized. However, these surfactants are not potent enough to fully stabilize the foam, therefore cross-linking agents are added to provide an added dimension of stability [58][59].

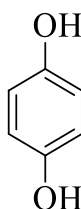
1.3.7 Auxiliary blowing agents

While the water-isocyanate reaction provides the primary blowing mechanism for flexible polyurethane foams, some products require the use of auxiliary blowing agents to achieve the desired level of density or softness. These blowing agents are low-boiling solvents which are inert in the chemical reactions already described in **Section 1.2**. As the highly exothermic foaming reactions proceed, the temperature in the mixtures reaches or exceeds 130 °C within two minutes. This large temperature increase is enough to vaporize the low boiling solvents, providing an additional amount of gas to expand the foam. The vaporization of these additional fluids does absorb a lot of the heat needed to expand the gas into the cellular structure; therefore, these formulations generally employ higher amount of catalyst needed to increase the amount of heat generated [60][61].

1.3.8 Additives

In order to achieve the desired product properties, it is sometimes necessary to include various additives. Some additives are used to make the product more appealing to consumers or to achieve a design specification. For example, colorants (metal oxides, carbon black, or dyes). We will use in one of the experimental studies the hydroquinone (structure shown in **Figure 30**). Other additives are included to improve product performance such as flame retardants, antistatic agents, bacteriostats, or UV stabilizers to prevent foams from yellowing. Finally,

some additives may be necessary for special applications. For example, plasticizers are used to reduce in-mold viscosity, cell-openers are used to enhance the cell wall rupture mechanisms, and compatibilizers are used to enhance emulsification beyond what the standard surfactant systems can achieve [62].



Hydroquinone

Figure 30: Chemical structure of hydroquinone.

2. Aims

The literature review revealed that polyurethane production is a complicated process and requires proper control of the reaction conditions. A better understanding of the reaction steps of the synthetic process can favor product optimization and help to find further solutions to the common technical problems encountered in laboratory and industrial applications, as well as to promote new technological developments. Hence, I would like to understand more deeply this complicated process with an atomistic view, according to the following stages:

- First, to better understand urethane bond formation at an atomistic level. I would like to study the known urethane bond formation in detail by using *ab initio* electronic structure calculations. The aim is to further determine the alternative reaction pathways of urethane bond formation for using either alcohol or isocyanate excess conditions in the liquid phase and to discover whether the alcohol or the isocyanate has the ability to self-catalyze the urethane bond formation.
- Secondly, I plan to conduct an experimental study on the kinetics of urethane bond formation to validate the results of the theoretical calculations from the first stage.
- Finally, I would like to extend the basic knowledge of urethane bond formation and apply it to polyurethane chemistry by modifying the reactants in the polyurethane synthesis. By adding mono-alcohols into the polyurethane formulation, I would like to determine whether it has a catalytic effect on polyurethane bond formation, I also aim to find out how the addition of the mono-alcohols can alter the mechanical properties of the polyurethane products.

The theoretical study of this reaction mechanism requires a robust quantum chemical protocol. In the same vein, the results from the electronic structure calculations guide us through the experimental investigations including a kinetic study using a microreactor and classical laboratory experiments on foam formation. This in turn, can provide us a piece of valuable information to understand the industrial reactions at the molecular level.

3. Materials and Methods

In this research, experimental and theoretical methods are combined to study polyurethane synthesis at the molecular level. Both procedures were used for the characterization of the urethane bond formation and polyurethane synthesis.

3.1 Materials

The isocyanates used in the reactions were the Ongronat® 2100, a polymeric MDI purchased from Wanhua-BorsodChem, and phenyl isocyanate (PhNCO) ($\geq 99\%$, Acros Organics), where the polyols used in our experiments are mostly polyether polyols based on glycerine such as Rokopol® M6000, Caradol® MC28-02, Alcupol® D-2021 and, PEG-600 purchased from Wanhua-BorsodChem. Mono-alcohols used in the reactions were methanol and isobutanol (Molar Chemicals), ethanol, 1-propanol, 2-propanol, 1-butanol, tert-butanol ($\geq 99\%$, VWR Chemicals), 1-hexanol and cyclohexanol (Alfa Aesar), 1-octanol (Scharlab Chemicals). Tetrahydrofuran (THF) ($\geq 99\%$, VWR Chemicals) solvent were stored over 20 %m/V activated molecular sieve (3Å, beads, VWR Chemicals) for at least two days to reach a low water content.[63]. Catalysts such as *N,N*-dimethylcyclohexylamine (DMCHA), triethylamine (TEA), diazabicycloundecene (DBU), *N*-methylmorpholine (NMM), *N*-ethylmorpholine (NEM), 1,4-diethylpiperazine (DEPP), and *n*-butylamine (BuA $\geq 99\%$) were purchased from erck. *N,N'*-diphenylurea (DPU $\geq 98\%$) was purchased from Alfa-Aesar.

3.2 Experimental methods

3.2.1 Kinetic and reactivity measurement of single urethane bond formation

Stock solutions of 2.0 M phenyl isocyanate (PhNCO) and 2.0 M propanol (PrOH) in THF (for the stoichiometric runs), and 4.0 M PhNCO, and 0.2 M PrOH in THF (for the NCO excess runs) were prepared in volumetric flasks. From the pre-incubated (± 0.1 °C) stock solutions, 5.0 mL of PhNCO and 5.0 mL of PrOH solutions were pipetted into a pre-incubated glass vial which was then capped. The experiments were conducted at 30, 40, and 50 °C. At different time intervals, a 10 μ l aliquot was withdrawn from the reaction mixture and mixed into 990 μ l ACN containing 30 μ l of *n*-butylamine in order to quench the reaction. The amine reacts spontaneously with the isocyanate to form the adduct, *N*-butylphenylurea. The quenched samples were further diluted by a factor of 50 (for the PhNCO excess runs) or 5 (for the stoichiometric runs) with ACN:H₂O=1:1 mixture and subjected to HPLC analysis. The concentration of *N,N'*-diphenylurea side-product (originating from the hydrolysis of PhNCO)

was also identified and was found to be a maximum of 5.6% of the starting PhNCO concentration. Further, the analytic detection technique was done on the quenched and diluted samples using a Shimadzu HPLC equipped with LC-20AD pumps, SIL-20AC autosampler, DGU-20A3R degassing unit, CTO-20A column oven, and SPD-M20A photodiode array detector. A SunShell C8 column (2.6 μm , 150 x 3.0 mm) equilibrated at 40 $^{\circ}\text{C}$ was used for the separation. The injection volume was 25 μl . The eluent was ACN:H₂O with a gradient as follows: 0–3.50 min, 42% ACN; 3.51–4.50 min, 82% ACN; 4.51–9.00 min, 42% ACN, at a flow rate of 0.6 $\text{mL}\cdot\text{min}^{-1}$. The product *n*-propyl phenylcarbamate was quantified at 239 nm. For calibration, the reference compound was synthesized from PhNCO in PrOH and purified by flash chromatography.



Figure 31: Microreactor setup: the Asia microflow system (Syrris Ltd., Royston, UK).

3.2.2 Synthesis of polyurethanes and mechanical properties analysis

To prepare flexible polyurethane foams, first, the polyol (Caradol MC28-02) was weighted with the given amount of monoalcohol, water, and catalyst (DMCHA) into a 500 mL plastic cup. Using a mechanical stirrer the mixture was stirred at 2000 rpm for 60 seconds at room temperature (22 ± 1 $^{\circ}\text{C}$). The amounts of the monool used were 0.2, 0.5, 1.0, and 2.0 parts by weight, which correspond to 0.2, 0.5, 1.0, and 2.0 w/w% of the polyol–monool mixture, respectively (Table 1). A reference foam without monoalcohol was also prepared. After the addition of the isocyanate (Ongronat 2100), the mixture was stirred at 3000 rpm for 10 seconds, and the foam was allowed to rise in the open cup. All recipes and calculations are based on 100 total parts by weight of polyol. The amount of other ingredients are normally listed as parts per

hundred parts of polyol by weight [64]. The quantity of the isocyanate in each formulation was based on the total hydroxyl content of the polyol and the monoalcohol. Water content, catalysts content, and isocyanate index (110) were kept constant. Foams were conditioned for 3 days at room temperature. All of the experiments have been repeated two times in order to test the reproducibility.

Functionality: The functionality of a B-side foam ingredient is the number of isocyanate reactive sites on a molecule. For polyols, the average functionality is generally used.

$$\text{Average Functionality} = \frac{\text{total moles OH}}{\text{total moles polyol}} \quad (1)$$

Hydroxyl Number (OH Number): the hydroxyl content of a polyol as determined by a wet analytical method. It is expressed as the milligrams of potassium hydroxide equivalent to the hydroxyl content in one gram of polyol or another hydroxyl compound.

$$\text{OH Number} = \frac{56.1 \times 1000}{\text{Equivalent Weight}} \quad (2)$$

Where 56.1 is the atomic weight of potassium hydroxide and 1000 is the number of milligrams in one gram of sample. The manufacturer provides the OH number for each lot of polyol.

Polyols are sometimes characterized by the weight percentage of hydroxyl groups. Conversion to hydroxyl number is accomplished by:

$$\text{OH Number} = 33 * \% \text{ OH} \quad (3)$$

Where the number 33 is obtained by the reduction of constants. For a mixture of polyols, the *hydroxyl number of the mixture* (OH_m) is given by:

$$\text{OH}_m = \text{OH Number}_A(\text{Wt. \% Polyol A}) + \text{OH Number}_B(\text{Wt. \% Polyol B}) + \dots \quad (4)$$

Equivalent Weight of a Polyol: The weight of a compound per reactive site.

$$\text{Equivalent Weight} = \frac{\text{Molecular Weight}}{\text{Functionality}} \quad (5)$$

After determining the parts of each polyol, (the total polyol parts should equal 100), we also determine the parts of other B-side components per 100 parts polyols, and finally take the sum of the parts of all B-side materials to get the total formula weight.

$$\text{Equivalents} = \frac{\text{Parts}}{\text{Equivalent Weight}} \quad (6)$$

After determining the equivalent weight of each B-side component, we can then calculate the equivalents of each B-side component such as water, catalysts, and other additives. In the end,

we can take the sum of the reactive equivalents of each B-side component to get the total B-side equivalents. Otherwise, the A-Side represents the amount of isocyanate required to react with the polyol, water, and other reactive additives that are calculated to give the desired stoichiometry. In actual practice, the amount of isocyanate is adjusted up or down depending on the particularity of the foam system.

Isocyanate Equivalent Weight: The equivalent weight (eq. wt.) is used to calculate how many grams of a product needed for one equivalent of reactive functional groups. For an isocyanate, the equivalent weight in isocyanate is the weight of a substance that contains 42.02 grams of the reactive group, which is NCO.

$$\text{Isocyanate equivalent weight} = \frac{42.02 \times 100}{\text{NCO Number}} \quad (7)$$

Isocyanate Index (NCO Index): The ratio of the equivalent amount of isocyanate used is relative to the theoretical equivalent amount times 100. The theoretical equivalent amount is equal to one equivalent isocyanate per one equivalent B-side compound.

$$\text{Isocyanate Index} = \frac{\text{Actual amount of Iso}}{\text{Theoretical Amount of Iso}} * 100 \quad (8)$$

After recording the isocyanate equivalent weight and selecting the desired NCO index, we can calculate the equivalent amount of *isocyanate parts required*.

$$\text{Eq. Iso} = \frac{(\text{Equivalents B-Side}) * (\text{Isocyanate Index})}{100} \quad (9)$$

$$\text{Parts Isocyanate} = (\text{Eq. Iso}) * (\text{Iso Eq. Wt.}) \quad (10)$$

We can also calculate the *B/A ratio* according to the following equation

$$\frac{B}{A} \text{ Ratio} = \frac{\text{Parts B-Side}}{\text{Parts A-Side}} \quad (11)$$

According to these calculations, we can now deduce the exact amount of each reagent needed in each experiment to produce the desired yield of polyurethane foam.

For the analysis of the compressive test and the density, samples having dimensions of 33 x 31 x 18 mm were cut from the prepared foams to measure the density and the compression properties of the foam. The density measurement is done by measuring the volume and the mass (the mass was determined by using an electronic weighing scale). The compression test was performed on an Instron(R) 5566 universal testing machine[65] using Instron compression plates (T1223-1021) with a diameter of 50 mm, with a 10 N or 10 kN load cell, at punch crosshead speeds (CHS) of 0.01–500 mm·min⁻¹. The testing was performed in a conditioned

room at 22 °C and 50% relative humidity, using a compression rate of 10 mm·min⁻¹. The specific compressive modulus and strength of polyurethane foam were measured at 83% deformation of the original height (18 mm) to be able to evaluate the material behavior over a large deformation interval (**Figure 32**). The computer related to the software can record the on-line load-displacement data after a quasi-static compression test. The acquired data is used for drawing the load-displacement curves (stress-strain diagram), from which the yield strength, compressive strength, and Young's modulus were determined.

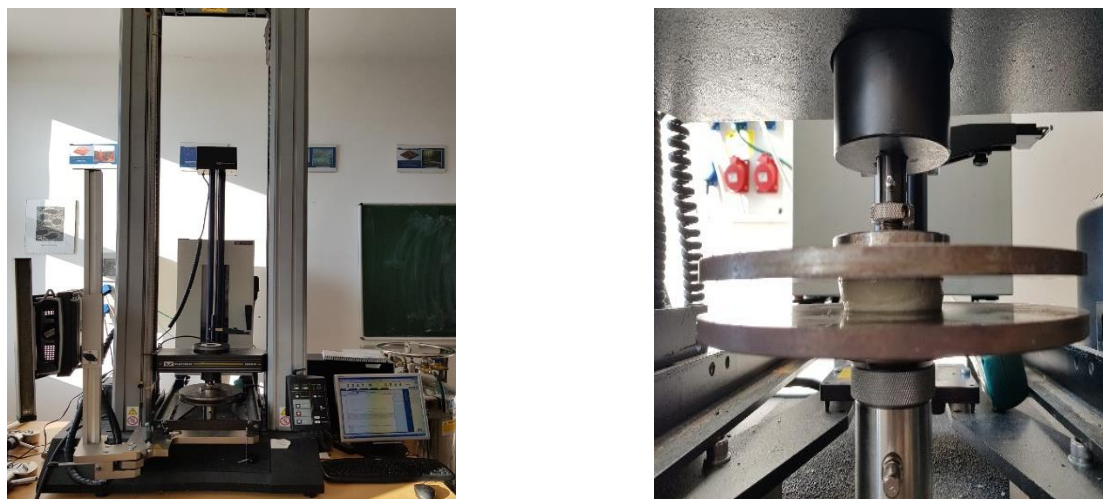


Figure 32: Compressive test of foam specimen with the Instron® 5566 universal testing machine.

3.3 Theoretical methods

Quantum chemistry has become a viable and powerful tool for solving problems related to chemical systems. The real prospect of quantum chemical computing is to supplement experiments as a means of discovering and exploring new chemistry. It uses computer simulations to predict the properties of new materials, even those that have not been synthesized in the laboratory. However, the calculation cost increases with the increase of the system size and the accuracy to be achieved. Improvements in computer performance and/or theoretical performance have made computational simulation an indispensable tool in materials science. Today, even in large and complex molecular systems, more results that are accurate can be gradually obtained within a reasonable time to determine the best structure defined as having the lowest possible energy. To obtain more accurate results of molecular properties, to be used in different applications, and to understand the physics of molecular systems, more reliable methods are needed [66]. The work reported in the thesis involves the use of quantum chemistry methods and experimental methods, to make a theory more closely mimic the experiment. One

has to consider not just one structure for a given chemical formula, but also all possible structures. That is, one characterizes the potential energy surface (PES) for a given chemical formula. Studies of the molecular, structural, vibrational, and energetic data of molecular systems are made either in the gas phase or solvent phase. Density functional theory (DFT) has been used to optimize the most stable molecules and to study the ground-state properties of the molecules studied. In any quantum chemical calculation, the first step requires optimization of the molecular geometry. It is customary to assume the system in the gas phase (isolated molecule). The wave functions and energy are computed for the initial guess of the geometry, which is then modified iteratively until the identification of energy minimum and ensuring that the forces within the molecules are zero. Using the optimized structure (minimum energy) molecular properties like polarizability, electron affinity, dipole moment, and the vibrational modes can also be calculated [67][68] by computing the second derivative of the energy concerning the pairs of the atomic Cartesian coordinates. Since an optimized geometry corresponds to zero forces within the molecule, all leading force constants must be positive (that is called reaction coordinate) and therefore should not result in any imaginary vibrational wavenumber. Some infinite properties that can be calculated by quantum chemistry methods, such as the calculation of optimized ground state and transition state structure (the potential energy), are molecular properties, vibrational wavenumbers, rotational constants, IR and Raman spectroscopy characterization of MO reactivity prediction, dipole moment, prediction of electronic excitation, UV spectrum, NMR spectrum, reaction rate, unpaired spin density, charge distribution and thermodynamic parameters $[G(T, p), E_0, S(T, p), H(T)]$. Through the thermodynamic functions, we calculate the most important macroscopic properties in experiments, such as heat of reaction ($\Delta_r H^\circ$), the heat of formation ($\Delta_f H^\circ$), heat capacity (C_v), Gibbs free energy ($\Delta_r G^\circ$), entropy (S) and acid dissociation constant (pK_a). From the macroscopic properties of molecules the reaction mechanism can be predicted, and by-products and side reactions can be evaluated.

3.3.1 Quantum Chemical Methods

Ab initio quantum chemistry methods are computational chemistry methods based on quantum chemistry.[69] The term *ab initio* indicates that the calculation is from first principles and that no empirical data is used. The quantum chemistry model is derived from the Schrödinger equation that first appeared in the late 1920s [70]. The solution of the Schrödinger equation depends on the movement of electrons, and it is directly related to the molecular structure and energy between other observables, and additionally contains key information of bonding.

Invoking the Born-Oppenheimer (BO) approximation [71] makes the Schrodinger equation easier to solve because the motion of electrons and nuclei can be separated due to their different masses. Therefore, quantum mechanical methods (*ab initio*, DFT, and semi-empirical methods) [72][73][74][75][76] are based on solving the time-independent Schrödinger equation related to the change of electrons in molecular systems over time and the position of the nucleus. In the classical atomistic model, atoms are regarded as basic units, and classical potential energy functions (force fields, FFs) represent the interactions between atoms.

Quantum chemical models differ from each other in the form and nature of these approximations and span a wide range in terms of consistency, capabilities, and computational cost. There are two different approaches to describe the electronic Schrödinger equation of atoms and molecules: **the wave function** and **density functional based methods**. The wave function-based method expands the electron wave function, which is the sum of Slater determinants, and optimizes the atomic orbitals and its coefficients through various numerical techniques. The simplest and most fundamental *ab initio* electronic structure calculation is the **Hartree-Fock (HF)** method.

- **The Hartree-Fock method** was first proposed in 1950 [77][78], on the premise that the N-body wave function of the system can be approximated by a single Slater determinant of N spin orbits [79]. It provides an appropriate description of equilibrium geometry, possible conformations, and provides good results for a variety of thermochemical comparisons.

Since electronic correlation is completely neglected, its use is limited. The wave function-based approach combining electron correlation is the **second-order Moller-Plesset (MP2)** perturbation theory [80]. Consider the perturbation sequence to include different numbers of items (ie, different orders) to apply. The second-order MP theory (MP2) is usually used for geometric optimization [81], while the fourth-order MP4 is used to refine the calculated energy. For example, the reason why the MP3 theory is used less frequently is that the effectiveness within the MP series tends to oscillate, so using even-numbered orders can give more consistent results. MP techniques are very commonly used due to the consistency of size and the better calculation efficiency [82].

The coupled-cluster (CC) perturbation theory and quadratic CI constitute another group of related techniques for considering electronic correlation [83]. These techniques represent the corrected wave function as the result of applying the so-called cluster operator to the HF wave function. The cluster operator may consist of a series of operators that consider the excitation

of one, two, three, or n electrons, where n is the total number of electrons in the molecule. Therefore, the CC technology can be truncated like the MP method, but with more accuracy. However, they are also more computationally expensive. CC calculations [84] using single and double excitation (CCSD) [85] are common, but usually, an additional perturbation term is used to consider triple excitations to give CCSD(T). The CCSD(T) calculation (or the closely related QCISD(T) technique) represents the best possible effect currently achieved using the HF wave function as a starting point (reference wave function) [86]. Each method has different computational scaling, depending on the number of electrons in the system.

Density functional theory (DFT) is an alternative to conventional quantum chemistry methods, implicit in terms of multi-electron wave functions, is mainly about the theory of the electronic ground state structure, using a wave function and the electron density to compute the energies [87]. The incorporation of the two Kohn-Sham (K-S) equations in 1965 made DFT lie on a solid theoretical foundation [88]. The first K-S theorem demonstrates that there is a one-to-one mapping between the ground state characteristics of a multi-electron system and its electron density. The second K-S theorem gives the concept of the energy function of the system and proves that the true ground-state electron density minimizes the energy functional. To solve the forces generated by electrons as they move around the nucleus, the K-S equation relies on a mathematical tool called an **exchange-correction functional**. Currently, many such functionals can be used to describe the electronic properties of matter. Presently, two main classes of functions have been widely deployed and tested in large-scale applications and small molecule benchmark tests: gradient-correction BLYP and hybrid B3LYP functions (Becke, 3-parameter, Lee-Yang-Parr) [89][90][91][92]. The gradient-correction functional starts with a local density approximation but adds terms related to the electron density gradient ($\nabla\rho$). The **hybrid functional** also includes gradient correction but adds an accurate Hartree-Fock exchange empirically built-in blending.

- **Composite methods** [93] The highest level of *ab initio* techniques are not suitable for medium-sized molecules (from a practical point of view) [94]. Two classes of approximations that overcome this difficulty are basis set extrapolation techniques and the design of composite methods. The former of these two classes is more accurate. It is based on the CCSD(T) calculations, extrapolates to the limit of the full basis set using a very large correlation-consistent basis set, and adds corrections for some smaller effects, which are not included in the calculation; for example, as the core valence effect, relativistic effect and atomic spin-orbit effect. This approach is limited to smaller molecules given a very large basis set must be used.

Composite methods are widely used in the calculation of thermochemical data. They combine accurate methods with smaller basis sets and less accurate methods with larger basis sets. They are often used to calculate thermodynamic quantities, such as enthalpy of formation, atomization energy, ionization energy, and electron affinity. The goal of employing these methods is to achieve chemical accuracy, usually defined as a deviation of less than 4.184 kJ·mol⁻¹ from the experimentally accepted value. One of the most popular is the Gaussian-n (Gn) theory, which as well use a set of calculations with different levels of accuracy and a basis set designed to approximate accurate energy. In the Gn approach, high-level correlation calculations (such as QCISD(T) and CCSD(T) with moderate-sized basis sets) are combined with energy from lower-level calculations with large base sets (such as MP4 and MP2), to approximate the energy of more expensive calculations. Besides, assuming that they are systematic, several empirical parameters independent of the molecule, such the higher-level correction (HLC) term, which are also included to estimate the remaining effects. All of these methods G1 [95], G2 [96], G3 [97], and G4 [98] are complex energy computations involving several pre-defined calculations on the specified molecular system. All of the distinct steps are performed automatically when one of these methods is specified, and the final computed energy value is displayed in the output. An intermediate approach has recently been introduced, called the correlation consistent composite approach (ccCA) with no parametrization [99][100]. Other composite techniques related to the Gn method include the complete basis set (CBS) methods [101][102][103] and the multi-coefficient method [104][105]. In the results and discussion section, I will focus on the G4MP2 quantum chemical protocol results [106]. In the case of this method, the geometry and zero-point energy are obtained from the B3LYP/6-31G(2df,p) level of theory at a scaled frequency of 0.96. [107]

3.3.2 Basis set

Two of the major methods (*ab initio* and DFT) require some understanding of basis sets and basis functions. The atom-centered functions used to describe the atomic orbitals are known as basis functions and collectively form a basis set. Larger basis sets give a better approximation to the atomic orbitals as the place fewer restrictions on the wave function which attract a higher computational cost. The STO-nG basis sets also exist and rather unsatisfactory as they include only one contracted Gaussian (CG) per atomic orbital. Where these basis sets approximate Slater-type orbitals (STOs) by n primitive Gaussians [108], *eg*: The STO-3G basis set is a minimal basis set where each atomic orbital is made up of 3 Gaussians. Split-valence basis sets model each valence orbital by two or more basis functions that have different exponents they

allow for size variations that occur in bonding. Examples include the double split-valence basis sets, 3-21G and 6-31G, and triple split-valence basis sets such as 6-311G. Polarisation functions have higher angular momentum, thus they are suitable for anisotropic variations that occur in bonding and help model the inter-electronic cusp. These include 6-31G(d) or 6-31G*, which included functions on the heavy atoms [109]. Diffuse basis functions are additional functions with small exponents, and are therefore large, thus they allow for accurate modeling of systems, Such examples include 6-31+G which has diffuse functions on the heavy atoms. Larger basis sets can be built up from these components, for example, 6-311++G(2df,2dp). Dunning basis sets also exist, for example, pVDZ and pVTZ. For larger atoms, Effective Core Potentials (ECPs) are often used. These replace the core electrons with an effective potential and have two main advantages: They reduce the number of electrons (cheaper), and they can be parameterized to take account of relativity. The valence electrons are still modeled using Gaussian type orbitals (GTOs) [110].

3.3.3 Solvation models

The use of implicit solvation models is nowadays one of the most adopted strategies to include the effect of the solvent into quantum mechanics (QM) calculations. These implicit solvation models place the molecule of interest into a cavity, whose surface charge is stabilized in accordance with the dielectric constant of the selected solvent, thus simulating the effect of the solute being exposed to the solvent. In this approach, the Solvation Model based on Density (SMD) allows accounting for the non-electrostatic contributions, not only regarding the energy but also the geometry optimizations and frequency calculations. It makes use of a smooth continuous model to assign charges on the molecular surface of the solute [111]. For SMD, the solute is polarizable by the charge density of the solvent and the interaction between the solute, and solvent can be determined via the charge density of the former and the electric polarization field of the latter. Moreover, SMD has proven to be an effective solvation model for use in both charged and uncharged systems and can predict accurate solvation energies for various functional groups, achieving an average mean absolute error of 16.7 kJ•mol⁻¹ in the solvation free energies of neutral species [112].

3.4 Applied computational methods

The theoretical part of the research was carried out by using different computational chemistry methods as implemented in the Gaussian09 program package[113]. In order to explore important reaction mechanisms, it is necessary to accurately characterize the structure of the

reactants, transition states (TS), complexes, intermediates (IM), and products. Preliminary calculations have been performed by using the B3LYP functional in combination with the 6-31G(d) basis set. As a refinement of the B3LYP/6-31G(d) level of theory, more robust and accurate composite methods from the Gaussian thermochemistry family were also applied such as the G3MP2B3, the G4MP2, and the CBS-QB3. For example, as part of the G3MP2B3 method by applying the “tight” convergence criterion. Normal mode analysis was performed on the optimized structures at the same level of theory to characterize their identities on the potential energy surface (PES). A transition state (TS) structure corresponds to a first-order saddle point on the potential energy surface (PES) and it is characterized by one imaginary vibrational mode (one negative frequency) [114]. Intrinsic reaction coordinate (IRC) calculations [115] were also tried to map out the minimal energy pathways (MEP), which means finding and confirming the minimum energy path between two assumed minima that connects reactants to products via the saddle point (transition state). Further single point quantum chemical calculations at the critical points of the PES were carried out using QCISD(T)/6-31G(d) (including MP2/6-31G(d) level of theory) and MP2/GTMP2 levels of theory based on B3LYP/6-31G(d) geometries according to the G3MP2B3 composite method [116][117]. G4MP2 calculations have also been carried out, in order to obtain accurate thermodynamic properties, such as zero-point corrected relative energy ($\Delta E_{0,G4MP2}$), relative enthalpy ($\Delta H_{0,G4MP2}$), relative Gibbs free energy ($\Delta G_{0,G4MP2}$), and entropy (S°). The heat of formation values have also been computed in gas phase at 1 atm of pressure (P) and $T = 298.15$ K ($\Delta H_{f,298.15K(g)}^\circ$) for the species involved in the studied reaction mechanisms. As part of the G4MP2 protocol, the B3LYP [118] functional was applied in combination with the 6-31G(2df,p) (noted as GTBas3 in Gaussian09 [113]) basis set for geometry optimizations using ‘tight’ convergence criteria and frequency calculations. The presence of solvent 1-propanol (PrOH, $\epsilon_r = 20.524$) as well as tetrahydrofuran (THF, $\epsilon_r = 7.4257$) has been mimicked, at each step of the G4MP2 protocol including geometry optimization and single point calculations, by using the SMD implicit solvation model. It has to be noted that the static relative permittivity for phenyl isocyanate (PhNCO, $\epsilon_r = 8.940$ [119]) is close to that of THF, therefore potential energy surface (PES) obtained in PhNCO and THF can be expected to be similar.

4. Results and Discussion

4.1 Urethane Formation at Isocyanate and Alcohol Excess

A kinetic and mechanistic investigation of the alcoholysis of phenyl isocyanate using 1-propanol as the alcohol was carried out. The mechanism of urethane formation in both excess alcohol and excess isocyanate have been studied (**Figure 33**). The experimental activation energies for the reactions of aryl isocyanates with alcohols are generally in the range of 17–54 $\text{kJ}\cdot\text{mol}^{-1}$. [120][121] For a given reaction, the activation energy depends on the solvent and the molar ratios of the reactants. Theoretical calculations were explored using a combination of accurate composite quantum chemical methods in combination with SMD implicit solvent model. They showed that a rather high energy barrier ($>100 \text{ kJ}\cdot\text{mol}^{-1}$) [122][123][124] is needed for reaching the bimolecular transition state (direct addition) and this barrier becomes substantially lower if one or two alcohol molecules (alcohol catalysis), or a urethane molecule (autocatalysis) are also incorporated in the transition state [122][125][126]. These mechanisms were analyzed from an energetic point of view. The kinetics of this reaction was also experimentally investigated by means of the analytical HPLC technique as described in **section 3.2.1**. From the rate constants measured at different temperatures, activation energies of the stoichiometric, the alcohol excess, and the isocyanate excess reactions were determined in **section 4.1.1**.

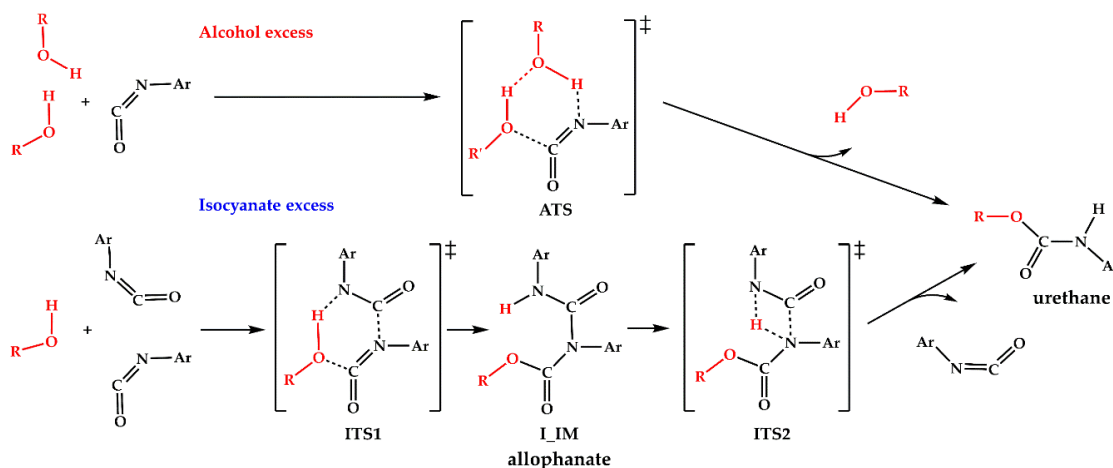


Figure 33: Reaction mechanism for urethane bond formation. Alcohol excess mechanism (top) involves hydrogen-bonded alcohol associate as reactant while isocyanate excess mechanism (bottom) starts with dipole-dipole stabilized intermolecular isocyanate dimer. In the present study R = propyl and Ar = phenyl.

4.1.1 Experimental results on kinetic of urethane bond formation

The rate constants (k_s for the stoichiometric reaction, $k_{I,obs}$ for the reaction running at 20-fold isocyanate excess) at different temperatures were determined by plotting the urethane concentration versus time (**Figure 33**) and applying a non-linear fitting using the kinetic equation **Equation 12** for second-order and **Equation 13** for pseudo-first-order reactions. For the latter, because of the 20-fold isocyanate excess, the isocyanate concentration during the reaction was regarded to be constant ($[PhNCO]_0$). This way the actual rate constant k_I can be calculated from the observed rate constant k_{obs} (**Equation 14**).

$$[urethane] = [PrOH]_0 \times \left(1 - \frac{1}{1 + [PrOH]_0 \times k_s \times t}\right) \quad (12)$$

$$[urethane] = [PrOH]_0 \times (1 - e^{-k_{I,obs} \times t}) \quad (13)$$

$$k_{I,obs} = k_I \times [PhNCO]_0 \quad (14)$$

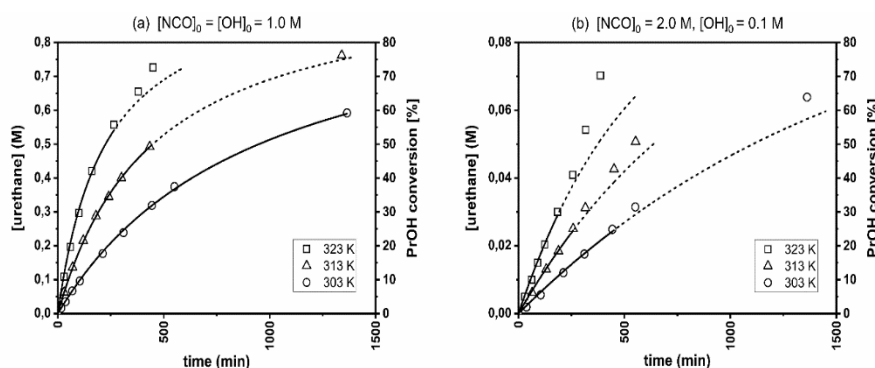


Figure 34: Experimental kinetic curves. (a) Second-order kinetics for the stoichiometric ratio (b) pseudo-first-order kinetics for the 20-fold PhNCO excess. Data points used for fitting and reaction rate constants determination are indicated by solid curve segments.

It is apparent from **Figure 34** that the first few data points fit well for the second-order equation **Equation 12** for **Figure 34(a)** and the pseudo-first-order equation **Equation 13** for **Figure 34(b)**, but at later reaction stages a positive deviation occurs which possibly accounts from urethane autocatalysis. In the case of the stoichiometric NCO/OH ratio, the addition reaction can be described by second-order kinetics up to 50–60% conversion. When the isocyanate is in 20-fold excess, the reaction follows pseudo-first-order kinetics only up to a conversion of 25–30%. Therefore, only the initial domain of the data (**Figure 34**) were used for non-linear fittings and reaction rate constant calculations. The kinetic parameters of the reactions were collected (**Table 3**). For the reaction in excess alcohol, the rate constants (k_A) and the activation energy were measured in the previous work of our group [121]. Using the Arrhenius equation and based on the kinetics parameters the Arrhenius plot was defined (**Figure 35**), where the activation energy for the reactions can be determined by finding the slope of the line.

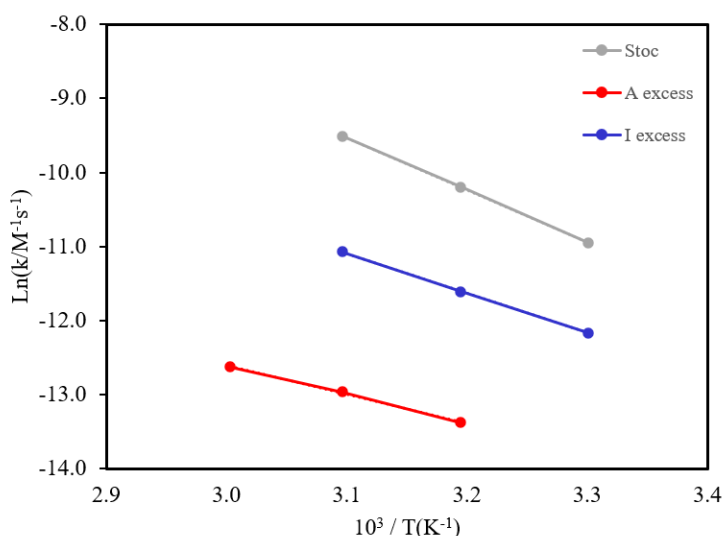


Figure 35: Arrhenius plots for stoichiometric (Stoc), alcohol excess (A excess) and isocyanate excess (I excess) reactions.

For both the alcohol and the isocyanate excess reactions the Arrhenius activation energies are lower than that of the stoichiometric reaction. From this, it is assumed that not only alcohol but also isocyanate molecules can also exert a catalytic effect and facilitate the reaction. At or near stoichiometric ratios both self-catalytic pathways can occur.

Table 3: Experimental reaction rate constants (k_A , k_S , and k_I) at different temperatures, Arrhenius activation energies (E_a), and pre-exponential factors (A). E_a and A values were obtained by the method of least squares. For $[NCO]_0 / [OH]_0 = 0.005$, data are taken from [121]. (*n.m.* = *not measured*)

Temperature, °C	Excess Alcohol [NCO] ₀ / [OH] ₀ = 0.005	Stoichiometric ratio [NCO] ₀ / [OH] ₀ = 1	Excess Isocyanate [NCO] ₀ / [OH] ₀ = 20
	$k_A \times 10^5, M^{-1} s^{-1}$	$k_S \times 10^5, M^{-1} s^{-1}$	$k_I \times 10^5, M^{-1} s^{-1}$
30	<i>n.m.</i>	1.76 ± 0.18	0.52 ± 0.04
40	0.16 ± 0.01	3.72 ± 0.32	0.91 ± 0.07
50	0.23 ± 0.01	7.41 ± 0.60	1.55 ± 0.11
60	0.33 ± 0.02	<i>n.m.</i>	<i>n.m.</i>
$E_a, kJ mol^{-1}$	30.4 ± 1.6	58.6 ± 6.0	44.2 ± 4.5
$A, M^{-1} s^{-1}$	18.8 ± 1.0	234113 ± 23971	214.9 ± 21.9

The rate constants in **Table 3** are the apparent rate constants, as the values depend on reaction conditions, such as the applied solvent and the concentrations of the reactants.

4.1.2 Reaction mechanisms based on theoretical calculations

Hydrogen bond stabilized alcohol associates are confirmed [127] and their role in reducing the activation energy in urethane formation has already been proved [122]. Furthermore, the thermodynamic values of the stationary points of the reactive potential energy surface are summarized in (**Table 4**) and relative zero-point corrected energies in 1-propanol (PrOH) and tetrahydrofuran (THF) are also displayed in (**Figure 36**). In this section I will focus only on the results of the G4MP2 calculation.

Table 4: G4MP2 thermochemical properties calculated in 1-propanol (PrOH) and tetrahydrofuran (THF) including zero-point corrected relative energies (ΔE_0), relative enthalpies ($\Delta H(T)$) and relative Gibbs free energies ($\Delta G(T,P)$) at $T = 298.15$ K, and $P = 1$ atm, **A** in excess alcohol, and **I** in excess isocyanate. All values are in $\text{kJ}\cdot\text{mol}^{-1}$.

Pathway	Species	ΔE_0		$\Delta H(T)$		$\Delta G(T,P)$	
		PrOH	THF	PrOH	THF	PrOH	THF
	PhNCO + 2 PrOH	0	0	0	0	0	0
Excess alcohol (A)	A_RC	-17.0	-30.8	-14.0	-27.2	25.1	50.5
	ATS	35.4	20.7	32.7	17.0	91.4	119.2
	A_PC	-99.7	-109.3	-100.9	-109.8	-47.4	-17.2
	2 PhNCO + PrOH	0	0	0	0	0	0
Excess isocyanate (I)	I_RC	-34.6	-12.7	-33.0	-11.1	-12.7	36.9
	ITS1	51.1	62.6	44.0	55.7	62.6	141.3
	I_IM	-152.3	-139.3	-160.1	-147.2	-139.3	-59.0
	ITS2	39.4	49.0	31.5	41.2	49.0	129.4
	I_PC	-105.6	-103.1	-109.2	-106.4	-103.1	-38.4

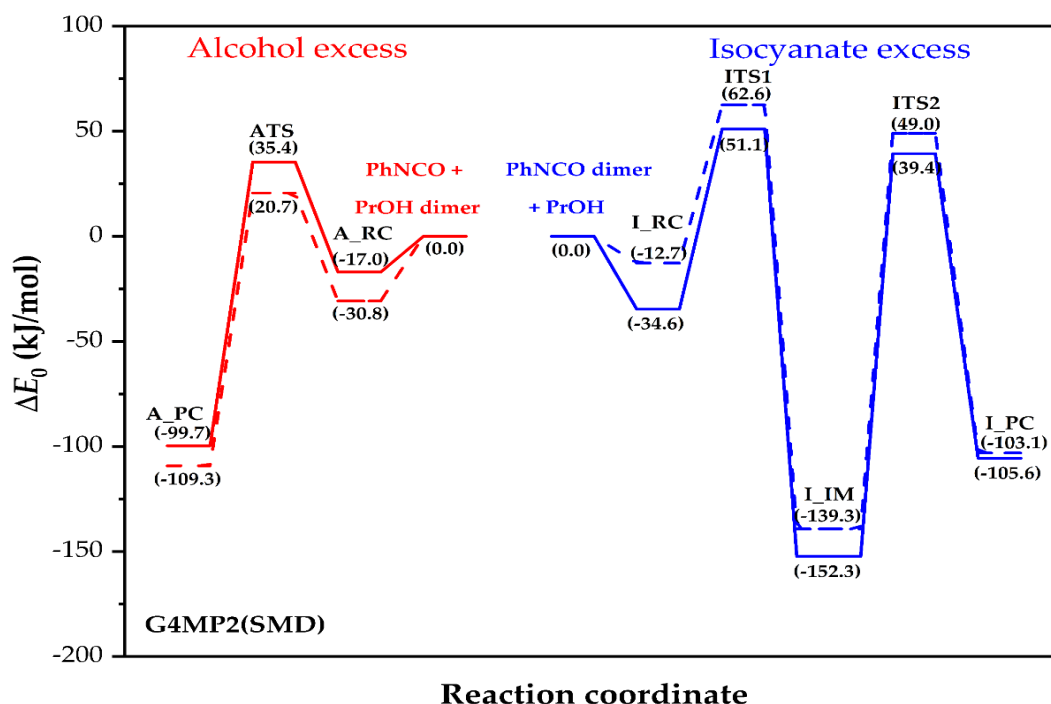


Figure 36: Energy profile (zero-point corrected) for the alcoholic route in 1-PrOH (red solid line), and in THF (red dashed line), and for the isocyanate route in 1-PrOH (blue solid line), and in THF (blue dashed line) calculated by using the G4MP2 composite method in combination with the SMD implicit solvent model.

In line with the theoretical and experimental work of Raspoet et al. [122], a reactive complex of the reaction in excess alcohol (A_RC) had been characterized and its structure is shown in **Figure 37**. This structure is stabilized by three strong hydrogen bonds between the molecular moieties, and the energy gain during the complex formation is $16.9 \text{ kJ}\cdot\text{mol}^{-1}$ in 1-propanol (PrOH) medium (values obtained in propanol solvent will be discussed further). In this concerted mechanism, the transition state structure (ATS in **Figure 37**) has a six-membered ring. In the ATS, the positively charged hydrogen of PrOH shifts to the electron-rich nitrogen of phenyl isocyanate (PhNCO), while the NCO group is bent, thereby activating the carbon for the formation of a new C-O bond with the other PrOH, and finally the hydrogen of the hydroxyl group is transferred to the other alcohol in the same time. Due to the complex interaction network the transition state energy is only $35.4 \text{ kJ}\cdot\text{mol}^{-1}$ above the reactant energy level, which is consistent with the theoretical value of $27.0 \text{ kJ}\cdot\text{mol}^{-1}$ (obtained at MP2/6-311++G(d,p)//MP2/6-31G(d,p) level of theory) reported by Raspoet et al. [122] for methanol and hydrogen isocyanate. As a result of the IRC calculation, the product complex (A_PC) had been also identified and the relevant structural parameters are displayed in **Figure 37**. As shown, the formed urethane bond is strongly hydrogen-bonded to the oxygen of the remaining PrOH. This exothermic reaction releases $99.7 \text{ kJ}\cdot\text{mol}^{-1}$ energy to form A_PC. Interestingly, the

relative energy of these stationary points becomes significantly lower by the changing the solvent from PrOH to THF. Obviously, the catalytic effect of the second alcohol can only be manifested when enough PrOH dimer is accessible to the reagents for the urethane formation reaction to take place.

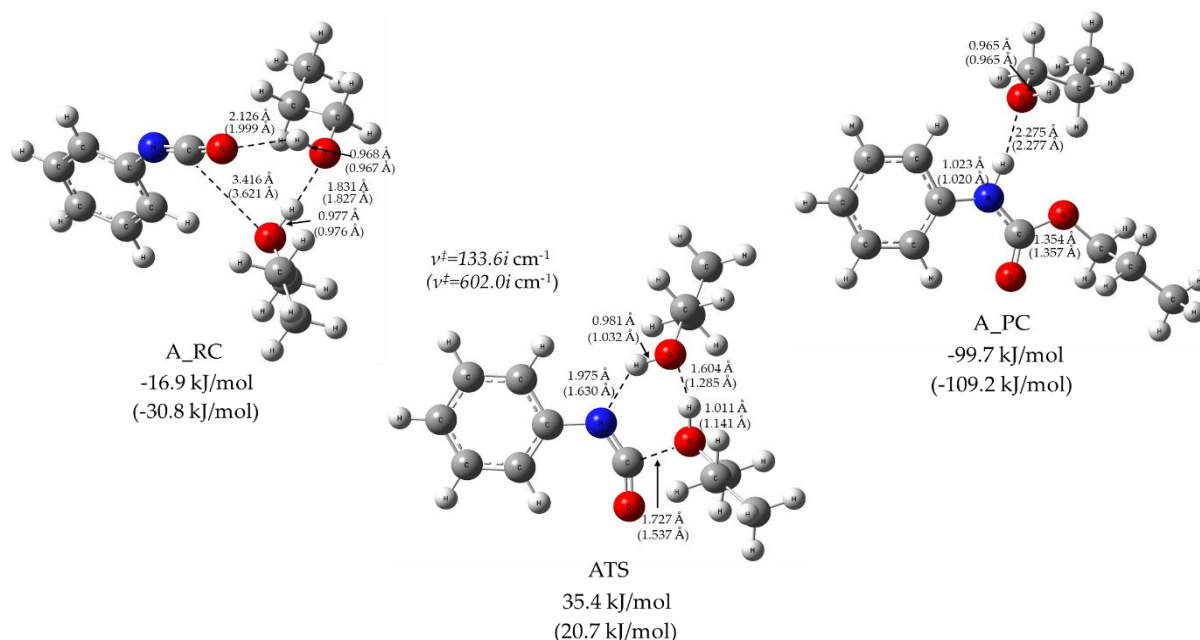


Figure 37: Reactive complex (RC), transition state structure (TS) and product complex (PC) structures (obtained at B3LYP/6-31G(2df,p) level of theory from G4MP2 calculation) for the excess alcohol reaction mechanism of urethane bond formation in solvent 1-PrOH or THF (in parenthesis). The relative zero-point corrected energies are also presented in kJ·mol⁻¹.

Despite the extensive use of PhNCO as a proxy in mechanistic studies for urethane formation, the physicochemical properties of liquid PhNCO are scarce in the literature. For example, only a schematic representation of the intermolecular interactions between PhNCO molecules can be found in the work of Baev [128] with an enthalpy of vaporization value ($\Delta H^\circ_{\text{vap}} = 46.5 \pm 0.3 \text{ kJ}\cdot\text{mol}^{-1}$), while viscosity and liquid structure of PhNCO to the best of our knowledge, were never reported. This $\Delta H^\circ_{\text{vap}}$ value is similar to that of 1-propanol ($\Delta H^\circ_{\text{vap}} = 47.5 \text{ kJ}\cdot\text{mol}^{-1}$) [129]. On the other hand, the viscosity of PhNCO is $0.96 \text{ mm}^2\cdot\text{s}^{-1}$ (298 K) according to our measurement, which is about 2.76 times smaller than that of 1-PrOH ($2.65 \text{ mm}^2\cdot\text{s}^{-1}$ at 298 K). It was proved in the literature based on accurate GAFF force field that the viscosity measured the interaction of the liquids, between propanol and phenyl isocyanate, in both cases could be similar to each other until then, as supported by the above mentioned $\Delta H^\circ_{\text{vap}}$. [128] [130] [131], one might hypothesize that the PhNCO dimers are stable enough to act as a reactant for the urethane formation under the condition of excess isocyanate.

The potential energy profile of the reaction which involves two phenyl isocyanate molecules with PrOH is shown in **Figure 36**. The reactive complex (I_RC) is stabilized by a hydrogen bond between the nitrogen of one of the PhNCO molecules and the hydroxyl of the PrOH molecule, as shown in **Figure 38**. In addition, the lone electron pairs of the hydroxyl point towards the positively charged carbon atom of the NCO group in the second PhNCO molecule with a distance of 2.992 Å. These interactions can significantly reduce the relative energy of the reactive complex ($-34.6 \text{ kJ}\cdot\text{mol}^{-1}$) compared to that of the reactants. The six-membered transition state structure (ITS1) resulted in the formation of an allophanate (I_IM), and has two synchronized bond-forming components that are combined with hydrogen abstraction, as shown in **Figure 38**. Here, both isocyanate groups are bent, and the new C-N bond being formed between the isocyanate groups is long (2.320 Å), while the critical distance between the alcohol oxygen and the isocyanato carbon is extremely small (1.519 Å). In the hydrogen abstraction component of the reaction coordinate, the moving hydrogen is attacked by the nitrogen of the isocyanato group from a relatively large distance ($r_{\text{H-N}} = 1.474 \text{ Å}$) and the O-H bond length is slightly elongated ($r_{\text{O-H}} = 1.067 \text{ Å}$). This motion also leads to the formation of a new C-O π -bond with a distance of 1.337 Å. ITS1 is $51.1 \text{ kJ}\cdot\text{mol}^{-1}$ higher in energy compared to the energy level of the reactants (PhNCO dimer and PrOH) and it is $15.7 \text{ kJ}\cdot\text{mol}^{-1}$ higher than the relative energy of ATS in the case of the excess alcohol mechanism.

As the IRC calculation starting from ITS1 confirmed, I_RC and I_IM are connected through ITS1. The formed allophanate (I_IM, propyl *N,N'*-diphenylallophanate) is a thermodynamically stable intermediate with the corresponding relative zero-point energy of $-152.3 \text{ kJ}\cdot\text{mol}^{-1}$. In its planar central structure, a strong intramolecular hydrogen bond can be found with a short H-O bond distance ($r_{\text{NH-O}} = 1.834 \text{ Å}$). According to the B3LYP/6-31G(2df,p) results, the N-H bond stretching mode and its rocking mode can be seen as intensive IR peaks at 3547.7 cm^{-1} and 1574.2 cm^{-1} , respectively. Furthermore, four additional high intensity IR wavenumbers can be assigned to the allophanate functional group. Symmetric and asymmetric C=O stretch modes are at 1761.2 cm^{-1} and 1713.7 cm^{-1} , respectively. The remaining two complex vibrational motions of the allophanate are at 1367.1 cm^{-1} and 1213.1 cm^{-1} . This IR spectral data may be used to monitor the components that take part in the reaction [132], although the assignment of these peaks can be difficult due to the multicomponent reaction mixtures as well as overlap amongst the IR peaks corresponding to similar functional groups (e.g. allophanate, biuret and urethane). Proper peak assignment for allophanates is still under debate [133].

Nevertheless, allophanate intermediates can further react through transition state ITS2 and lead to the urethane–phenyl isocyanate complex I_PC. As can be seen in **Figure 38**, ITS2 is a tight, four-membered transition state corresponding to a hydrogen shift from one of the allophanate nitrogen to the other. Comparing the relative energy of ITS1 and ITS2, ITS1 is found to be a bottleneck of these reaction channels since all thermodynamic parameters are higher for ITS1 than for ITS2 by at least 11.8 kJ·mol⁻¹ as shown in **Table 4**. In contrast to the mechanism in excess propanol, in the excess isocyanate mechanism a change in the solvent (from PrOH to THF) increased the relative energy, enthalpy, and Gibbs free energy values, also seen in **Table 4**.

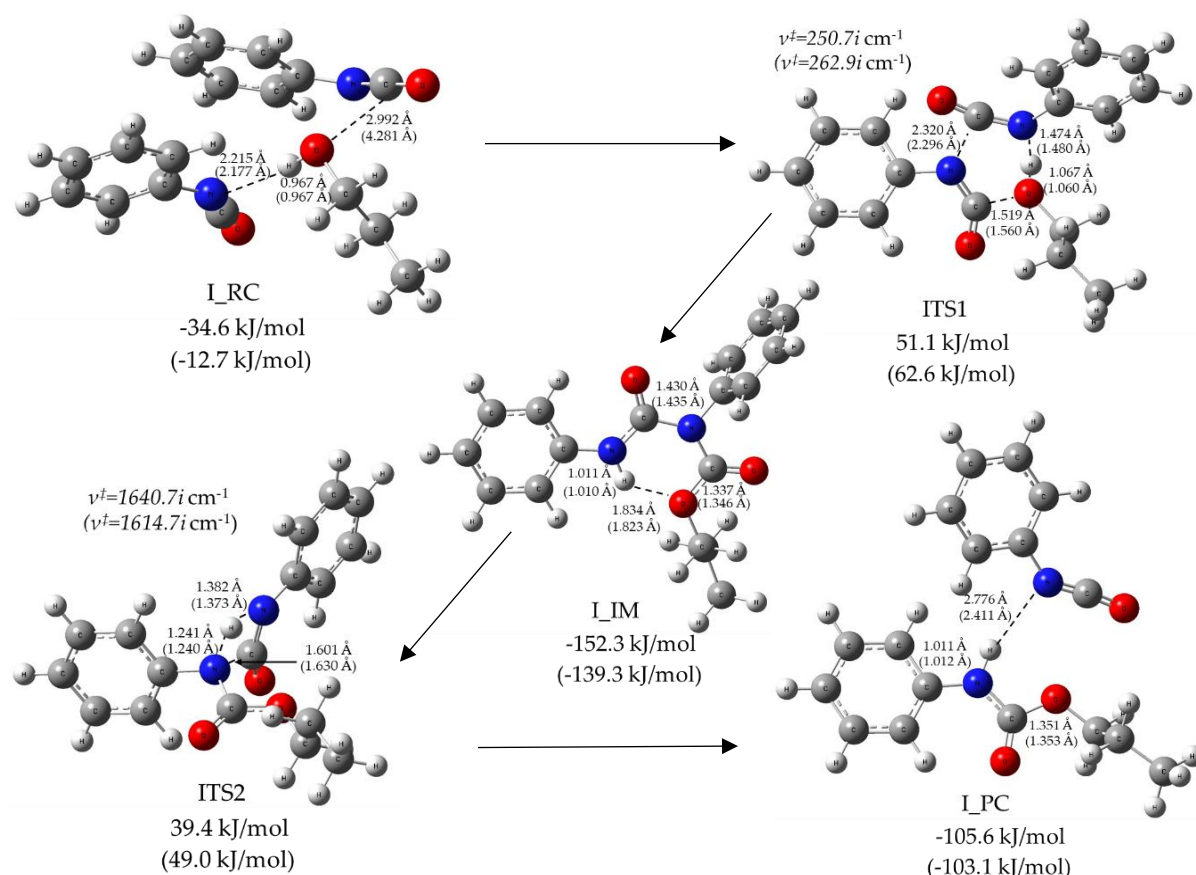


Figure 38: Reactive complex (RC), transition state structure (TS), intermediate (IM) and product complex (PC) structures (obtained at B3LYP/6 31G(2df,p) level of theory from G4MP2 calculation) for the isocyanate excess reaction mechanism of urethane bond formation in solvent 1-PrOH or THF (in parenthesis). The relative zero-point corrected energies are also presented in kJ·mol⁻¹.

Allophanate formation in excess isocyanate has been already reported [134], although the previously proposed reaction mechanism started from a covalently bonded, cyclic isocyanate dimer (uretidione) which then react with alcohol to give allophanate. Allophanate can then decompose to urethane and isocyanate. In contrast to this, our proposed mechanism only assumes the formation of the non-covalent dimer, which can react with alcohol through a low-

lying, six-membered transition state to form an allophanate intermediate. This transition state is structurally similar to the proposed one at alcohol excess condition. The results above lead us to the first and second thesis points.

Composite method test

I used the B3LYP function combined with the 6-31G(d) basic set to explore all the systems. In order to improve on the theoretical level of B3LYP/6-31G(d), more powerful composite methods such as G3MP2B3, G4MP2, and CBS-QB3 have been studied, with the purpose of comparing them and choose the more accurate one with precise thermodynamic properties, and good performance, with respect to the experimental result. **Table 5** shows the comparison of different barrier energies of different methods and the experimental results. We could express the Arrhenius activation energy (E_a) in terms of the standard enthalpy of activation (ΔH) and the temperature with Equation 15:

$$E_a = \Delta H + 2RT \quad (15)$$

Table 5: Relative enthalpies of all the transition state of the reaction at excess alcohol and excess isocyanate, obtained with different methods of calculation ($\Delta H(T)$) at $T = 298.15$ K, and $P = 1$ atm, calculated in 1-propanol (PrOH) comparing to the experimental Arrhenius activation energies (E_a) and calculated (E_a^{G4MP2}), ATS according to alcohol excess, and ITS1 to isocyanate excess. All values are in $\text{kJ} \cdot \text{mol}^{-1}$.

Species	$\Delta H(T)$ (PrOH)				E_a^{G4MP2}	E_a	$STDEV$
	G4MP2	G3MP2B3	CBS-QB3	B3LYP	Calc.	Exp.	E_a
ATS	32.7	33.0	19.6	32.9	37.7	30.4	5.1
ITS1	44.0	40.6	91.3	63.5	49.0	44.2	3.4

From **Table 5** I compared the experimental and calculated Arrhenius activation energies. The mechanism that is proposed with G4MP2 quantum chemical protocol in the 1-propanol solvent fits very well with the experimental results and has an excellent agreement, and can be considered the best composite method. These results lead us to the third thesis point.

Proposing this new catalytic mechanism of urethane formation in both alcohol and isocyanate excess, we notice that the energy profile of alcohol excess reaction has a lower barrier energy and a faster reaction comparing to isocyanate excess. Based on theoretical and experimental results, our study reveals a new possible mechanism for urethane formation, wherein two isocyanate molecules facilitate the formation of the product. Besides this new, isocyanate-catalyzed trimolecular mechanism, the applied G4MP2 composite quantum chemical method (with SMD implicit solvent model) also supports the already known hypothesis for alcohol self-

catalysis. While the alcohol-catalyzed route turned out to be a one-step process, the isocyanate-catalyzed path includes two reaction steps, including the formation of an allophanate intermediate. The key step of the new mechanism is the 1,3-H shift between the nitrogen atoms of the allophanate. The potential energy surface (PES) highly depends on the applied solvent. This is in agreement with the well-known solvent dependence of the kinetics of urethane formation. The experimental finding, i.e. lower activation energies for either the alcohol or the isocyanate-excess reactions compared to the stoichiometric reaction also suggests that both self-catalytic pathways are feasible.

4.2 Polyurethane bond formation

The previous study concluded that the structure of the polyol (alcohol) component has a significant impact on the formation process. In this part of the study, I added monoalcohols into the polyurethane formulation to determine whether an excessive amount of alcohol has an effect on polyurethane bond formation during the polymerization process. The amount of these monoalcohols used for chain modification were comparable to that of the catalyst, to see if they have a catalytic effect or have an influence on other properties.

The properties of polyurethane foams are strongly influenced by the chain length, molecular weight, functionality, and hydroxyl value of the polyol [135][136]. This study aims to use monoalcohols as active additives in polyurethane foam synthesis to obtain products with high quality in terms of resistance. The use of monoalcohols has been highlighted in several patents, and this work aims to prepare polyurethanes or polyisocyanurate–polyurethane polymers that have, for example, low density, good heat adhesive properties to fibrous materials, or low viscosity with good flow characteristics. [130 and references to other patents therein]. The density range of flexible polyurethane foam based on polyether or polyester polyol is (10 – 800 kg·m⁻³). In this new study, various monoalcohols are used to decrease the average molecular weight of the polyurethane. They were added to the starting components at different concentrations in order to prepare polyurethanes with modified characteristics, while keeping the other factors in the foam formulation such as water content, catalysts, and isocyanate index constant. the quantity of the isocyanate in each formulation was based on the total hydroxyl content of Caradol MC28-02 and the monoalcohol. The foam formulation for modified flexible polyurethane foam is shown in **Table 6**. The addition of a small amount of the monoalcohols into Caradol MC28-02 has a small influence on the OH number of the mixture. With 7% for

the largest molecular weight monool, which is the 1-octanol. The hydroxyl number of mixture (OH_m) is given by the flowing **Equation 16** [138].

$$OH_m = OH_j * a + OH_k * (1 - a) \quad (16)$$

Hydroxyl numbers of compounds (OH_j , OH_k) and fractional weights part of each component (a) and $(1 - a)$, where (j: Caradol MC28-02 and k: monoalcohol).

Table 6: The components and the typical concentration used in the production of modified flexible polyurethane foam.

Component	Parts by Weight			
B-side materials				
Caradol® MC28-02	99.8	99.5	99.0	98.0
Monoalcohol	0.2	0.5	1.0	2.0
Blowing Agent (distilled water)			1.8	
DMCHA			1.2	
A-side material				
Ongronat® 2100			37.0 – 47.0	

The monoalcohol reacts with the isocyanate function, blocking it from further reactions with the polyol (**Figure 39**).

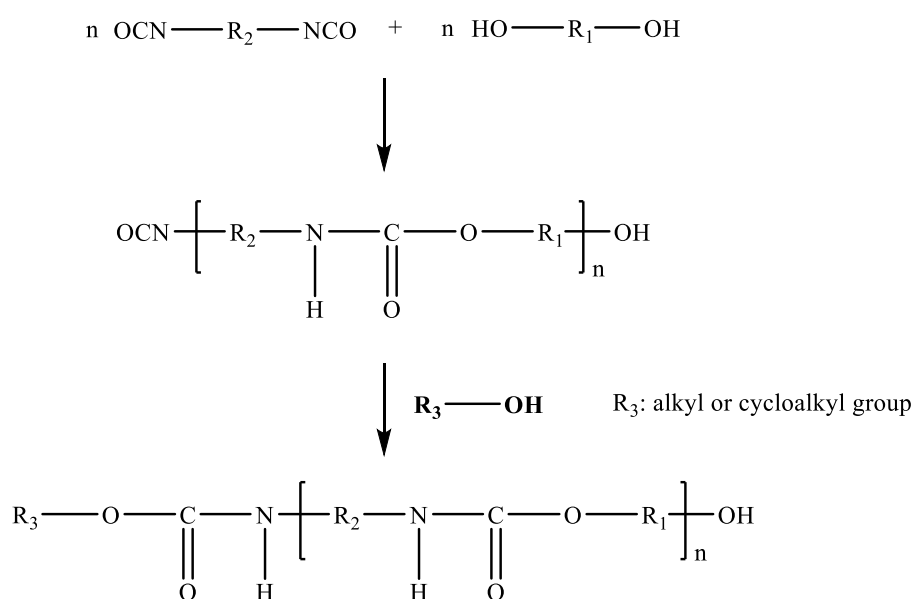


Figure 39: Polyurethane synthesis modified by a monoalcohol ($R_3\text{-OH}$).

Ten commercially available monoalcohols have been selected and tested in the concentration range of 0.2, 0.5, 1.0, and 2.0 parts by weight (pbw) (**Figure 40**).

The density and compressibility of the foams have been measured and compared. All the characteristics were compared to a reference foam synthesized without any monoalcohol.



Figure 40: Flexible polyurethane foams, all with the concentration of monoalcohol in the range of 0.2, 0.5, 1.0, and 2.0%.

3.2.1 Effect of mono-alcohols on polyurethane bond formation

a. Foam height

Figure 41 demonstrates the effect of monoalcohol content on the height of PU foams. Increasing the chain length of the monoalcohols leads to an increase in the height of the foam, furthermore, the height of the foams increases with increasing concentration of the monoalcohols, providing an additional degree of freedom to control the foam volume, which may otherwise be affected by the lower boiling point and volatility of these monoalcohols.

Based on the inspection, monoalcohols appear to be more effective at forming foam in which the volume of the foams is much greater than the initial foaming of the reference without the addition of monoalcohols.

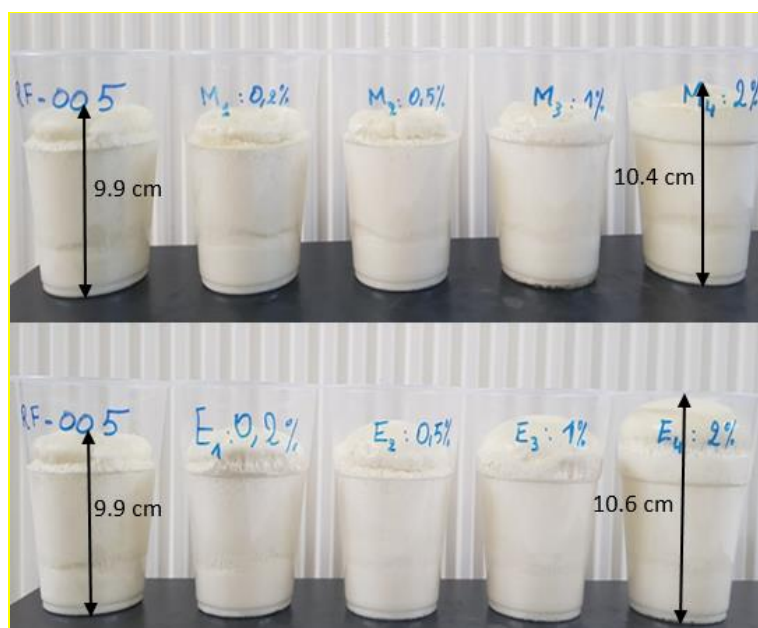


Figure 41: Height of flexible polyurethane foams with methanol and ethanol at concentrations of 0.2, 0.5, 1.0, 2.0%.

b. Foam density

The results demonstrate that with increasing concentration of monoalcohol, the density of the foam depends on the number of carbon atoms in the alcohol (chain length) (**Figures 42 and Figure 43**).

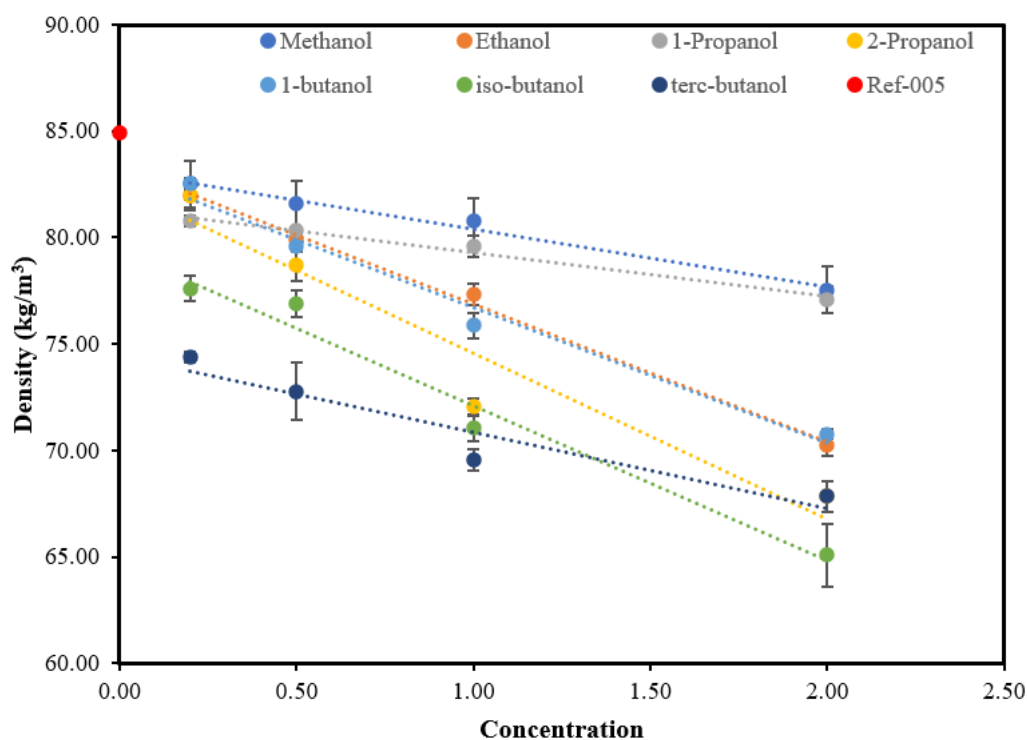


Figure 42: Densities of polyurethane foams as a function of monoalcohol concentration.

Figure 42 describes the densities of polyurethane foams as a function of monoalcohol concentration, with chain length from C1 to C4, regardless of chain type (straight or branched), the density of the foam decreases as the concentration of alcohol increases. In all cases, the density is lower than that of the reference foam ($84.9 \text{ kg}\cdot\text{m}^{-3}$). Among the tested alcohols, when methanol, ethanol, 1-propanol, 2-propanol, or 1-butanol were used in 0.2 pbw, the densities are similar ($81\text{--}82 \text{ kg}\cdot\text{m}^{-3}$). Besides the alcohol concentration increases, the density values start to decrease. At 2.0 pbw, the densities are 82–90 % lower compared to the reference foam.

In the case of 0.2 pbw isobutanol, *tert*-butanol (**Figures 42**), 1-hexanol, cyclohexanol, or 1-octanol (**Figures 43**) the densities are in the range of $74\text{--}77 \text{ kg}\cdot\text{m}^{-3}$. Isobutanol and *tert*-butanol behave like the other butanol isomers, namely increasing their concentration leads to a decrease in density, which, at 2.0 pbw corresponds to 75–80 % of the density of the reference foam. When using 1-hexanol, cyclohexanol, or 1-octanol, an opposite trend is seen: as the concentration increase, the densities also increase, however, at 2.0 pbw the foams still have a lower density than that of the reference.

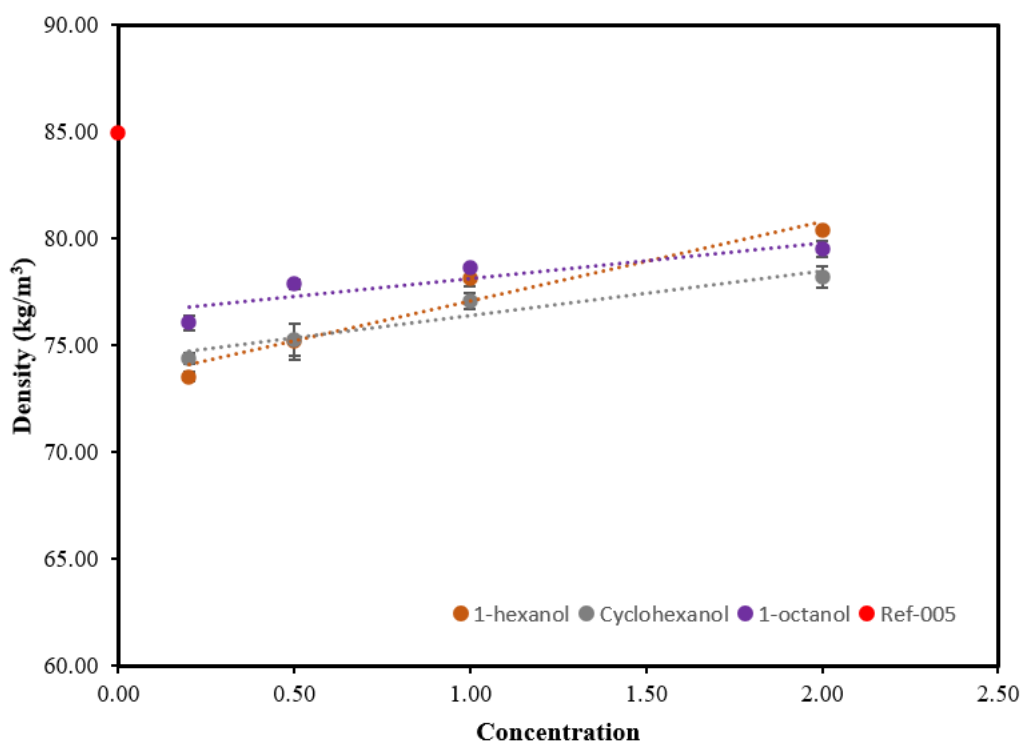


Figure 43: Densities of polyurethane foams as a function of monoalcohol concentration

c. Mechanical properties

Table 7 presents the Young's modulus and the density of the prepared polyurethane foams with different monoalcohols at different concentrations (0.2, 0.5, 1.0, and 2.0).

Table 7: Density and mechanical properties of polyurethane flexible foams.

mono-alcohols	Concentrations	density AVERAGE	density STDEV	Young's modulus AVERAGE	Young's modulus STDEV
	pbw	kg/m ³	kg/m ³	GPa	GPa
Reference	-	84.94	0.00	7.74E-05	0.00E+00
Methanol	0.20	82.52	0.24	2.99E-05	1.98E-07
Methanol	0.50	81.57	0.37	5.64E-05	2.62E-07
Methanol	1.00	80.79	0.24	7.40E-05	5.85E-06
Methanol	2.00	77.55	1.02	8.30E-05	1.85E-05
Ethanol	0.20	82.00	0.24	4.12E-05	6.08E-07
Ethanol	0.50	79.93	0.24	4.56E-05	1.84E-07
Ethanol	1.00	77.34	0.49	3.21E-05	5.94E-07
Ethanol	2.00	70.26	0.49	4.31E-05	1.87E-06
1-Propanol	0.20	80.79	0.24	4.30E-05	2.06E-06
1-Propanol	0.50	80.36	0.12	4.82E-05	4.24E-06
1-Propanol	1.00	79.59	0.49	4.53E-05	3.08E-06
1-Propanol	2.00	77.08	0.61	3.21E-05	2.82E-06
2-propanol	0.20	82.00	0.73	4.02E-05	6.15E-07
2-propanol	0.50	78.72	0.73	2.98E-05	6.36E-08
2-propanol	1.00	72.08	0.37	3.79E-05	9.48E-07
2-propanol	2.00	67.85	0.73	5.49E-05	3.50E-06
1-butanol	0.20	82.52	0.24	4.17E-05	8.41E-06
1-butanol	0.50	79.59	0.24	3.41E-05	1.44E-05
1-butanol	1.00	75.87	0.61	3.42E-05	5.79E-06
1-butanol	2.00	70.78	0.24	3.20E-05	3.03E-06
iso-butanol	0.20	77.60	0.61	6.14E-05	2.44E-05
iso-butanol	0.50	76.91	0.61	5.80E-05	4.00E-05
iso-butanol	1.00	71.04	0.61	7.48E-05	9.90E-06
iso-butanol	2.00	65.08	1.46	2.84E-05	1.23E-05
terc-butanol	0.20	74.41	0.24	4.21E-05	1.04E-06
terc-butanol	0.50	72.77	1.34	4.59E-05	1.98E-07
terc-butanol	1.00	69.57	0.49	5.89E-05	1.18E-05
terc-butanol	2.00	67.85	0.73	5.81E-05	4.50E-05
1-hexanol	0.20	73.54	0.24	4.81E-05	2.01E-05
1-hexanol	0.50	75.18	0.85	5.50E-05	7.30E-06
1-hexanol	1.00	78.12	0.37	4.54E-05	1.51E-06
1-hexanol	2.00	80.36	0.12	5.23E-05	2.26E-06
Cyclohexanol	0.20	74.41	0.24	4.68E-05	1.70E-07
Cyclohexanol	0.50	75.27	0.73	6.36E-05	1.53E-06
Cyclohexanol	1.00	77.08	0.37	5.45E-05	3.13E-06
Cyclohexanol	2.00	78.20	0.49	4.65E-05	6.04E-06
1-octanol	0.20	76.05	0.37	5.33E-05	2.12E-06
1-octanol	0.50	77.86	0.24	4.74E-05	1.66E-05
1-octanol	1.00	78.64	0.12	4.77E-05	2.57E-05
1-octanol	2.00	79.50	0.37	4.50E-05	1.02E-06

From (**Table 7**), a relation between density and Young's modulus can be distinguished, presented according to the Ashby plot that is a scatter plot, which displays two or more properties of many materials or classes of materials [139]. These plots are useful to compare the ratio between different properties. An example of the stiffness/lightness ratio discussed above, which would have Young's modulus on one axis and density on the other, with one data point on the graph for each candidate material. On such a plot, it is easy to find not only the material with the highest stiffness, or that with the lowest density, but that with the best E/ρ ratio. Using a log scale on both axes facilitates the selection of the material with the best plate stiffness.

The benefit of this study allows us to define our target on producing optimal flexible polyurethane foams, where the cost is not the only important factor in material selection. The key design objective was the stiffness of a plate of the material, where we are looking for an optimal combination of density and Young's modulus that provides us to study the relation between these two parameters in our diagram. **Figure 44** presents a plot of Young's modulus vs density of the results with log scaling on the ordinate.

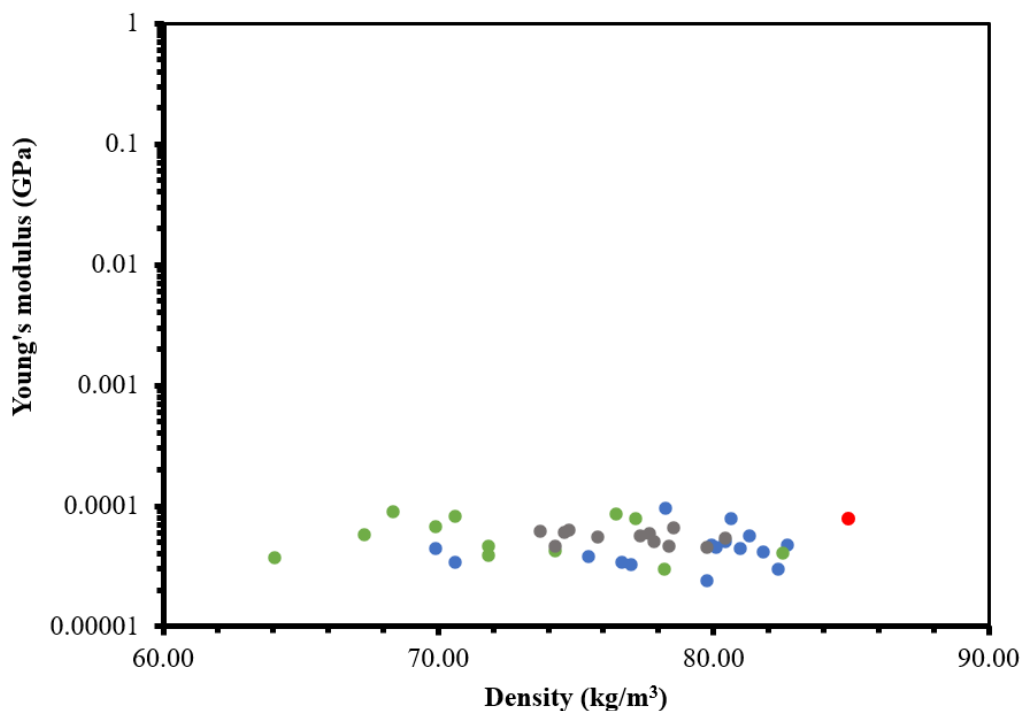


Figure 44: The Plot of Young's modulus vs density.

From the results of the diagram presented in **Figure 44**, we illustrate a new range for Young's modulus values between (0.0001–0.00002 GPa). This range is completely new compared to the recent research in the case of flexible foams (see **Figure 45**). Whereas the range of density is

almost the same as other recently published results. The gray dots represent the long-chain alcohols, $\geq C_6$, they are centered between blue and green with the density range between 73–80 $\text{kg}\cdot\text{m}^{-3}$. Moreover, the green dots are mainly represented on the right side with a density range between 64–82 $\text{kg}\cdot\text{m}^{-3}$. These correspond to the branched-chain with chain length $\leq C_4$, since for the blue dots the majority are represented on the left side, they correspond to the straight chain with chain length $\leq C_4$, the density range is along between 70–85 $\text{kg}\cdot\text{m}^{-3}$.

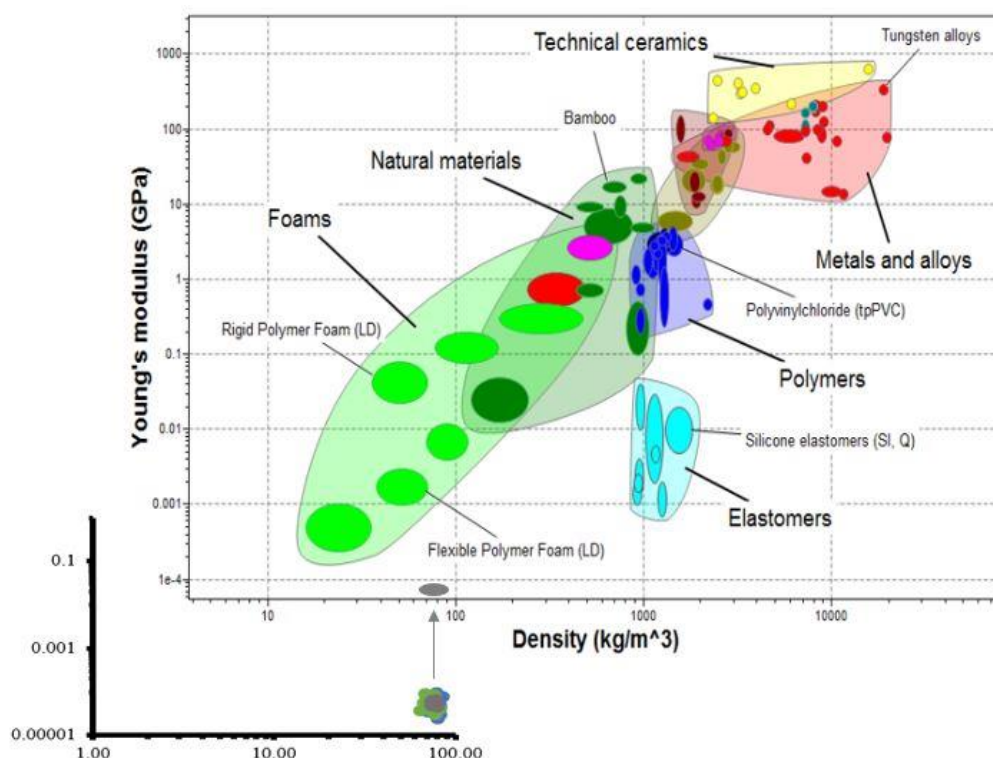


Figure 45: A chart of Young's modulus and density for materials created using the CES EduPack 2007 software with the Level 2 database.

The results showed that the addition of different monoalcohols as a second reactive component in the polyurethane composition affects the selected properties of the obtained material. PU foams were prepared with a high concentration of monoalcohols containing a maximum of four carbon atoms with a straight-chain and branched-chain; they decrease the density of the foams, whereas the monoalcohols having a high chain length of more than six carbons increase the density. The mechanical properties of these PU foams change with the density. By increasing the concentration of the monoalcohols, the results from the compressive test show us a low deformation of the flexible PU foams, which is due to the high flexibility of the material. The use of monoalcohols could be a good alternative for a wide range of industrial applications in the production of polyurethanes. Whereby the above results lead us to the fourth and fifth thesis points.

5. Summary

Polyurethane products are inseparable from our daily life. They are practically everywhere and are readily available. Polyurethane synthesis is a complex process. By fine tuning the ratio of reactants and additives, polyurethane products can be produced with a wide range of properties. The purpose of this research was to study the urethane bond formation and polyurethane synthesis at the molecular level. Urethane bond formation occurs through a reaction between an isocyanate and alcohol and is an essential component of the polyurethanes. In this work, the direct formation of a urethane bond between an aromatic isocyanate (phenyl isocyanate) and an aliphatic alcohol (1-propanol) was investigated. Theoretical and experimental studies were combined, and the reaction mechanism of urethane bond formation was investigated using *ab initio* calculations and analytical methods.

The kinetics of the reaction were studied experimentally using analytical HPLC. From the rate constants measured at different temperatures and using the Arrhenius equation, activation energies corresponding to stoichiometric, excess alcohol, and excess isocyanate reactions were determined. The activation energies for both the excess alcohol reaction and the excess isocyanate reaction were lower compared to the stoichiometric reaction ($30.4 \pm 1.6 \text{ kJ}\cdot\text{mol}^{-1}$, $44.2 \pm 4.5 \text{ kJ}\cdot\text{mol}^{-1}$, and $58.6 \pm 6.0 \text{ kJ}\cdot\text{mol}^{-1}$, respectively).

The quantum chemical G4MP2 method in combination with the implicit SMD solvent model was chosen for the calculations, and the results of the calculated activation energies of ATS and ITS1 were in good agreement within $5.1 \text{ kJ}\cdot\text{mol}^{-1}$, and $3.4 \text{ kJ}\cdot\text{mol}^{-1}$, respectively, of the average absolute deviation corresponding to the experimental data. The reaction mechanisms were studied in excess alcohol and excess isocyanate. A new two-step mechanism for isocyanate excess has been proposed, in which allophanate is an intermediate towards urethane formation via a six-membered transition state (TS) with a barrier of $62.6 \text{ kJ}\cdot\text{mol}^{-1}$ in THF solvent. In the next step, a synchronous 1,3-H shift between the nitrogens of the allophanate and the cleavage of the C-N bond led to the release of the isocyanate and the formation of the urethane bond via a low-lying TS with $49.0 \text{ kJ}\cdot\text{mol}^{-1}$ relative energy. Theoretical calculations showed that the energy required for either the alcohol- or isocyanate-catalyzed pathway is lower compared to the stoichiometric (bimolecular) mechanism (**Figure 35**).

The urethane linkage is inevitable for polyurethane formation, and the results of the first study can be used for a deeper understanding of polymer synthesis. The importance of the alcohol component has been shown and it was also found that the polymerization can be significantly

changed by the presence of excess alcohol. Therefore, the properties of polyurethane foams are strongly influenced by the chain length and molecular weight of the molecules added to the system. Monoalcohols are capable of decreasing the molecular weight of the polyurethane product and increasing the occurrence of the chain breaking. Different monoalcohols (from methanol to 1-octanol) have been used as a second alcohol in polyurethane foam synthesis and their effect on the mechanical behavior of the foams has been investigated. The additional monoalcohol concentrations were also varied between 0.2 to 2.0 parts by weight. The compressive strength and density of the foams have been measured and it was found that the length of the monoalcohol chain, especially with a shorter carbon chain, opened a way to produce lighter polymers with only slight changes in mechanical properties in the preparation of flexible polyurethane foams. Moreover, increasing the concentration of the monoalcohol increased the flexibility of the polyurethane product. Furthermore, the obtained results show a new range of Young's modulus values between 0.0001-0.00002 GPa, meanwhile the density range is almost the same as in the case of other published materials. Compared to the literature results of flexible foams, a completely new range of properties was obtained in the present study (see **Figure 44**).

6. Thesis point

Based on our combined experimental and theoretical study of polyurethane synthesis, the following main conclusions were drawn as new scientific results:

1st thesis

A new reaction mechanism of urethane bond formation has been proposed in the case of excess alcohol and excess isocyanate in the liquid phase. Based on *ab initio* calculations and experimental measurements, it was proved that both the alcohol and the isocyanate can self-catalyze the urethane bond formation.

2nd thesis

The alcohol-catalyzed route was shown to be a one-step process, whereas the isocyanate-catalyzed pathway includes two consecutive reaction steps. The route in excess alcohol is more favorable, as a lower barrier height have been found compared to the isocyanate route. In the case where neither the alcohol nor the isocyanate were in excess, the energy barrier was the highest.

3rd thesis

The experimental Arrhenius parameters for both catalytic routes are in excellent agreement with the calculated ones.

- I found the activation energies for the alcohol-catalyzed route measured and calculated equal to $30.4 \pm 1.6 \text{ kJ}\cdot\text{mol}^{-1}$ and $37.7 \text{ kJ}\cdot\text{mol}^{-1}$, respectively.
- For the isocyanate-catalyzed mechanism I found that the activation energy measured and calculated is equal to $44.2 \pm 4.5 \text{ kJ}\cdot\text{mol}^{-1}$ and $49.0 \text{ kJ}\cdot\text{mol}^{-1}$, respectively.

4th thesis

An experimental study was carried out to determine whether the addition of monoalcohols has an extra catalytic effect on polyurethane bond formation. The reference system were primarily catalyzed by 1.2 % DMCHA. The addition of the same amount of monoalcohol does not causes extra catalytic effect.

We are concluding that the monoalcohols as self-catalysts are weaker compared with the tertiary amine DMCHA.

5th thesis

It was found that the addition of monoalcohols could affect the density and the Young's modulus of the foam. A new range of properties in the Ashby plot has been achieved.

7. Scientific publications

Publication bibliometrics

Number of papers: 3

Cumulative impact factor related to the thesis: 5.455

Total number of citations: 9

Scientific publications

1. Wafaa Cheikh, Zsófia Borbála Rózsa, Christian Orlando Camacho López, Péter Mizsey, Béla Viskolcz, Milán Szőri, Zsolt Fejes, Urethane Formation with an Excess of Isocyanate or Alcohol: Experimental and Ab Initio Study, *Polymers*, doi: 10.3390/polym11101543. (Q1; IF = 3.426)
2. Boros Renáta Zsanett, Koós Tamás, Wafaa Cheikh, Nehéz Károly, Farkas László, Viskolcz Béla, Szőri Milán, A theoretical study on the phosgenation of methylene diphenyl diamine (MDA), *Journal chemical physics letters*, doi: 10.1016/j.cplett.2018.06.024. (Q2; IF = 2.029)
3. Wafaa Cheikh, Zsolt Fejes, Béla Viskolcz, Light polyurethane flexible foams by using monoalcohol–polyol mixtures, *submitted*

Oral and Poster presentations

1. 9th Visegrad Symposium on Structural Systems Biology, systematic molecular design, Szilvásvárad, Hungary, 2019, *Oral presentation*.
2. The 6th International Scientific Conference on Advances in Mechanical Engineering, Experimental study of polyurethane foams synthesis, Debrecen, Hungary, 2018, *Oral presentation*
3. The Scientific Conference for Ph.D. Students, The effect of mono-alcohols and diols on the properties of polyurethane foams, Miskolc, Hungary, 2018, *Poster*
4. XXIII. Bolyai Konferencián conference, Effect of different mono-alcohols on polyurethane foams, Budapest, Hungary, 2018, *Poster*
5. 7th Visegrad Symposium on Structural Systems Biology, Computational study of the phosgenation reaction mechanisms of the MDA, Nove Hrad, Czech Republic, 2017, *Poster*

8. References

- [1] G. Woods, *The ICI Polyurethanes book*. Published jointly by ICI Polyurethanes and Wiley, 1990.
- [2] P. Król, “Synthesis methods, chemical structures and phase structures of linear polyurethanes. Properties and applications of linear polyurethanes in polyurethane elastomers, copolymers and ionomers,” *Progress in Materials Science*, vol. 52, no. 6, pp. 915–1015, Aug-2007.
- [3] P. Deepa and M. Jayakannan, “Solvent-free and nonisocyanate melt transurethane reaction for aliphatic polyurethanes and mechanistic aspects,” *J. Polym. Sci. Part A Polym. Chem.*, vol. 46, no. 7, pp. 2445–2458, Apr. 2008.
- [4] J. W. Dieter and C. A. Byrne, “Aliphatic polyurethane elastomers with high performance properties,” *Polym. Eng. Sci.*, vol. 27, no. 9, pp. 673–683, 1987.
- [5] M. Farhan, T. Rudolph, U. Nöchel, K. Kratz, and A. Lendlein, “Extractable Free Polymer Chains Enhance Actuation Performance of Crystallizable Poly(ϵ -caprolactone) Networks and Enable Self-Healing,” *Polymers (Basel)*, vol. 10, no. 3, p. 255, Mar. 2018.
- [6] A. Bouilloux, C. W. Macosko, and T. Kotnour, “Urethane Polymerization in a Counterrotating Twin-Screw Extruder,” *Ind. Eng. Chem. Res.*, vol. 30, no. 11, pp. 2431–2436, Nov. 1991.
- [7] G. Hinrichsen, “Polyurethane handbook,” *Acta Polym.*, vol. 45, no. 5, pp. 398–398, Oct. 1994.
- [8] A. M. Heintz, D. J. Duffy, S. L. Hsu, W. Suen, W. Chu, and C. W. Paul, “Effects of reaction temperature on the formation of polyurethane prepolymer structures,” *Macromolecules*, vol. 36, no. 8, pp. 2695–2704, Apr. 2003.
- [9] M. Ionescu, *Chemistry and Technology of Polyols for Polyurethane Volume 2*, vol. 2. Rapra Technology, 2016.
- [10] D. Randall and S. Lee, *The polyurethanes book*. [Huntsman Polyurethanes], 2002.
- [11] D. Klempner, K. C. Frisch, and J. H. Saunders, *Handbook of Polymeric Foams and Foam Technology edited by*. 1991.

- [12] F. Saint-Michel, L. Chazeau, J.-Y. Cavaillé, and E. Chabert, “Mechanical properties of high density polyurethane foams: I. Effect of the density,” *Compos. Sci. Technol.*, vol. 66, p. 66, 2006.
- [13] R. H. Harding, “Relationships Between Cell Structure and Rigid Foam Properties,” *J. Cell. Plast.*, vol. 1, no. 3, pp. 385–394, Jul. 1965.
- [14] A. Bîrca, O. Gherasim, V. Grumezescu, and A. M. Grumezescu, “Introduction in thermoplastic and thermosetting polymers,” *Mater. Biomed. Eng. Thermoset Thermoplast. Polym.*, pp. 1–28, 2019.
- [15] UNEP TEAP, *Handbook for the Montreal Protocol on Substances that Deplete the Ozone Layer*. United Nations Environment Programme PO Box 30552-00100 Nairobi Kenya : Secretariat for the vienna convention for the protection of the ozone layer, the montreal protocol on substances that deplete the ozone layer , 2016.
- [16] Kyoto Protocol, “United Nations Framework Convention on Climate Change (UNFCCC),” *Am. J. Int. Law*, vol. 92, no. 2, pp. 315–331, 1997.
- [17] S. K. Goel and E. J. Beckman, “Generation of microcellular polymeric foams using supercritical carbon dioxide. I: Effect of pressure and temperature on nucleation,” *Polym. Eng. Sci.*, vol. 34, no. 14, pp. 1137–1147, Jul. 1994.
- [18] S. K. Goel and E. J. Beckman, “Generation of microcellular polymeric foams using supercritical carbon dioxide. II: Cell growth and skin formation,” *Polym. Eng. Sci.*, vol. 34, no. 14, pp. 1148–1156, Jul. 1994.
- [19] E. Di Maio, G. Mensitieri, S. Iannace, N. L., W. Li, and R. W. Flumerfelt, “Structure optimization of polycaprolactone foams by using mixtures of CO₂ and N₂ as blowing agents,” *Polym. Eng. Sci.*, vol. 45, no. 3, pp. 432–441, Mar. 2005.
- [20] E. Reverchon and S. Cardea, “Production of controlled polymeric foams by supercritical CO₂,” *J. Supercrit. Fluids*, vol. 40, no. 1, pp. 144–152, Feb. 2007.
- [21] R. Herrington and K. Hock, *Flexible polyurethane foams*, 2nd ed. Midland: Dow Chemical, 1997.
- [22] M. V. Pandya, D. D. Deshpande, and D. G. Hundiware, “Effect of diisocyanate structure on viscoelastic, thermal, mechanical and electrical properties of cast polyurethanes,” *J. Appl. Polym. Sci.*, vol. 32, no. 5, pp. 4959–4969, Oct. 1986.

- [23] K. Ashida, *Polyurethane and Related Foams*. CRC Press, 2006.
- [24] F. N. Jones, M. E. Nichols, and S. P. Pappas, *Organic Coatings*. Hoboken, NJ, USA: John Wiley & Sons, Inc., 2017.
- [25] T. C. Wen, S. S. Luo, and C. H. Yang, “Ionic conductivity of polymer electrolytes derived from various diisocyanate-based waterborne polyurethanes,” *Polymer (Guildf)*, vol. 41, no. 18, pp. 6755–6764, Aug. 2000.
- [26] M. Malik and R. Kaur, “Influence of aliphatic and aromatic isocyanates on the properties of poly(ether ester) polyol based PU adhesive system,” *Polym. Eng. Sci.*, vol. 58, no. 1, pp. 112–117, Jan. 2018.
- [27] H. Ulrich, *Chemistry and Technology of Isocyanates*. New York: John Wiley & Sons, 1997.
- [28] S. J. Moravek and R. F. Storey, “Reaction kinetics of dicyclohexylmethane-4,4'-diisocyanate with 1- And 2-butanol: A model study for polyurethane formation,” *J. Appl. Polym. Sci.*, vol. 109, no. 5, pp. 3101–3107, Sep. 2008.
- [29] A. M. I and W. R. J. J, “Kinetic and statistical aspects of the formation of polyurethanes from toluene diisocyanate.,” *Polymer (Guildf)*, vol. 27, no. 3, pp. 425–430, 1986.
- [30] Í. Yilgör and J. E. McGrath, “Effect of catalysts on the reaction between a cycloaliphatic diisocyanate (H-MDI) and n-butanol,” *J. Appl. Polym. Sci.*, vol. 30, no. 4, pp. 1733–1739, Apr. 1985.
- [31] M. Gambiroža-jukić, Z. Gomzi, and H. J. Mencer, “Kinetic analysis of bulk polymerization of diisocyanate and polyol,” *J. Appl. Polym. Sci.*, vol. 47, no. 3, pp. 513–519, 1993.
- [32] P. Król and J. Wojturska, “Kinetic study on the reaction of 2,4- and 2,6-tolylene diisocyanate with 1-butanol in the presence of styrene, as a model reaction for the process that yields interpenetrating polyurethane-polyester networks,” *J. Appl. Polym. Sci.*, vol. 88, no. 2, pp. 327–336, Apr. 2003.
- [33] H. Ni, H. A. Nash, J. G. Worden, and M. D. Soucek, “Effect of catalysts on the reaction of an aliphatic isocyanate and water,” *J. Polym. Sci. Part A Polym. Chem.*, vol. 40, no. 11, pp. 1677–1688, Jun. 2002.

- [34] G. Woods, *Flexible polyurethane foams : chemistry and technology*. Applied Science Publishers, 1982.
- [35] J. H. Saunders and K. C. Frisch, *Polyurethanes : chemistry and technology. Part I, Chemistry*. New-York; Londres: Interscience Publishers, 1962.
- [36] J.-C. Berthier, "Polyuréthanes PUR," *Ref TIP100WEB - "Plastiques Compos.*, Jan. 2009.
- [37] K. Dusek, M. Spirkova, and I. Havlicek, "Network formation of polyurethanes due to side reactions," *Macromolecules*, vol. 23, no. 6, pp. 1774–1781, 1990.
- [38] A. Lapprand *et al.*, "Reactivity of isocyanates with urethanes: Conditions for allophanate formation," *Polym. Degrad. Stab.*, vol. 90, pp. 363–373, 2005.
- [39] Frank Richter, Andreas Hecking, and Reinhard Halpaap, "Preparation of uretdione polyisocyanates," 2009.
- [40] Robert L Hansen, "Carbodiimide catalysts and processes," 1973.
- [41] A. Williams and I. T. Ibrahim, "Carbodiimide Chemistry: Recent Advances," *Chem. Rev.*, vol. 81, no. 6, pp. 589–636, 1981.
- [42] C. Hepburn and C. Hepburn, "Chemistry and Basic Intermediates," in *Polyurethane Elastomers*, Springer Netherlands, 1992, pp. 1–28.
- [43] E. Sharmin and F. Zafar, "Polyurethane: An Introduction," in *Polyurethane*, InTech, 2012.
- [44] Mark F. Sonnenschein, *Polyurethanes: Science, Technology, Markets, and Trends*. Midland, MI, USA: John Wiley & Sons, 2014.
- [45] Y. Li, X. Luo, and S. Hu, "Introduction to Bio-based Polyols and Polyurethanes," 2015, pp. 1–13.
- [46] M. Ionescu, *Chemistry and technology of polyols for polyurethanes*. Rapra Technology, 2005.
- [47] G. Shkapenko, G. T. Gmitter, and E. E. Gruber, "Mechanism of the Water-Isocyanate Reaction," *Ind. Eng. Chem.*, vol. 52, no. 7, pp. 605–608, Jul. 1960.
- [48] F. Hostettler and E. F. Cox, "Catalysts for Urethane Technology ... Organotin

- Compounds in Isocyanate Reactions,” *Ind. Eng. Chem.*, vol. 52, no. 7, pp. 609–610, Jul. 1960.
- [49] D. Ihms, J. Stoffer, D. Schneider, and C. McClain, “Effect of Catalysts on the Kinetics of the Water-toluene Diisocyanate Reaction,” *J. Coatings Technol.*, Jan. 1985.
- [50] V. de Lima, N. da Silva Pelissoli, J. Dullius, R. Ligabue, and S. Einloft, “Kinetic study of polyurethane synthesis using different catalytic systems of Fe, Cu, Sn, and Cr,” *J. Appl. Polym. Sci.*, vol. 115, no. 3, pp. 1797–1802, Feb. 2010.
- [51] S.-W. Wong and K. C. Frisch, “Catalysis in competing isocyanate reactions. I. Effect of organotin–tertiary amine catalysts on phenyl isocyanate and N-butanol reaction,” *J. Polym. Sci. Part A Polym. Chem.*, vol. 24, no. 11, pp. 2867–2875, Nov. 1986.
- [52] N. Malwitz, S. W. Wong, K. C. Frisch, and P. A. Manis, “Amine Catalysis of Polyurethane Foams,” *J. Cell. Plast.*, vol. 23, no. 5, pp. 461–502, 1987.
- [53] H. Okada and Y. Iwakura, “The kinetics of the polyurethane-forming reaction between organic diisocyanates and glycols. II,” *Die Makromol. Chemie*, vol. 66, no. 1, pp. 91–101, Jan. 1963.
- [54] M. Gambiroza-jukic, Z. Gomzi, and H. J. Mencer, “Kinetic analysis of bulk polymerization of diisocyanate and polyol,” *J. Appl. Polym. Sci.*, vol. 47, no. 3, pp. 513–519, Jan. 1993.
- [55] L. THIELE and R. BECKER, “Catalytic mechanisms of polyurethane formation,” *Adv. urethane Sci. Technol.*, vol. 12, 1993.
- [56] R. Van Maris, Y. Tamano, H. Yoshimura, and K. M. Gay, “Polyurethane Catalysis by Tertiary Amines,” *J. Cell. Plast.*, vol. 41, no. 4, pp. 305–322, Jul. 2005.
- [57] X. D. Zhang, C. W. Macosko, H. T. Davis, A. D. Nikolov, and D. T. Wasan, “Role of silicone surfactant in flexible polyurethane foam,” *J. Colloid Interface Sci.*, vol. 215, no. 2, pp. 270–279, Jul. 1999.
- [58] Gamini Ananda Vedage, Juan Jesus Burdeniuc, J. Allen Robert Arnold, and James Douglas Tobias, “Crosslinkers for improving stability of polyurethane foams,” 17-Oct-2013.
- [59] Y. Luo, J. Zou, J. Li, H. Zou, and M. Liang, “Effect of crosslinking agent on properties

- and morphology of water-blown semirigid polyurethane foam,” *J. Appl. Polym. Sci.*, vol. 135, no. 42, p. 46753, Nov. 2018.
- [60] J. G. Burt and D. F. Brizzolara, “Auxiliary Blowing Agents for Flexible Polyurethane Foams,” *J. Cell. Plast.*, vol. 13, no. 1, pp. 57–61, Jan. 1977.
- [61] R. M. Hennington, V. Zellmer, and M. Klincke, “Soft Flexible Polyurethane Foam without Auxiliary Blowing Agents,” *J. Cell. Plast.*, vol. 27, no. 4, pp. 337–353, 1991.
- [62] Wolfgang Fischer, Thomas Hattich, William Krug, and Gerhard Schuster, “Process for producing articles made from polyurethane foam and additive for performing this process,” 06-Nov-1986.
- [63] D. B. G. Williams and M. Lawton, “Drying of organic solvents: Quantitative evaluation of the efficiency of several desiccants,” *J. Org. Chem.*, vol. 75, no. 24, pp. 8351–8354, 2010.
- [64] E. K. Moss, “Computer Calculation of Urethane Foam Permutations,” *J. Cell. Plast.*, vol. 5, no. 5, pp. 282–288, 1969.
- [65] Instron 5500 Manual, “Instron Series 5500 Load Frames Reference Manual,” 2005.
- [66] R. A. Friesner, “Ab initio quantum chemistry: Methodology and applications,” *Proc. Natl. Acad. Sci. U. S. A.*, vol. 102, no. 19, pp. 6648–6653, 2005.
- [67] L. Sinha, O. Prasad, V. Narayan, and R. K. Srivastava, “Electronic structure, non-linear properties and vibrational analysis of Acenaphthene and its carbonyl derivative Acenaphthenequinone by density functional theory,” *J. Mol. Struct. THEOCHEM*, vol. 958, no. 1–3, pp. 33–40, Oct. 2010.
- [68] A. Kumar, V. Narayan, O. Prasad, and L. Sinha, “Monomeric and dimeric structures, electronic properties and vibrational spectra of azelaic acid by HF and B3LYP methods,” *J. Mol. Struct.*, vol. 1022, pp. 81–88, Aug. 2012.
- [69] Ira N. Levine, *Quantum Chemistry*, no. 7. 2013.
- [70] H. F. Schaefer, “A history of ab initio computational quantum chemistry: 1950-1960,” *Tetrahedron Comput. Methodol.*, vol. 1, no. 2, pp. 97–102, Jan. 1988.
- [71] M. Born and R. Oppenheimer, “On the quantum theory of molecules,” *Ann. Phys.*, vol. 389, no. 20, pp. 457–484, Jan. 1927.

- [72] Warren J. Hehre, Leo Radom, Paul von R. Schleyer, and John Pople, *Ab Initio Molecular Orbital Theory*. New York: Wiley, 1986.
- [73] A. Szabo and N. S. Ostlund, *Modern quantum chemistry : introduction to advanced electronic structure theory*. New York: Macmillan, 1982.
- [74] P. Atkins and R. Friedman, *Molecular quantum mechanics*, 4th ed. New York: Oxford university press, 2005.
- [75] Robert G Parr and Weitao Yang, *Density-functional theory of atoms and molecules*. New York: Oxford University Press, 1989.
- [76] Walter Thiel, "Semiempirical quantum-chemical methods in computational chemistry," *Theory Appl. Comput. Chem.*, pp. 559–580, 2005.
- [77] D. R. Hartree, "The Wave Mechanics of an Atom with a Non-Coulomb Central Field Part I Theory and Methods," *Math. Proc. Cambridge Philos. Soc.*, vol. 24, no. 1, pp. 89–110, 1928.
- [78] D. R. Hartree, "The Wave Mechanics of an Atom with a Non-Coulomb Central Field Part I Theory and Methods," *Math. Proc. Cambridge Philos. Soc.*, vol. 24, no. 1, pp. 89–110, 1928.
- [79] C. C. J. Roothaan, "New developments in molecular orbital theory," *Rev. Mod. Phys.*, vol. 23, no. 2, pp. 69–89, Apr. 1951.
- [80] C. Møller and M. S. Plesset, "Note on an approximation treatment for many-electron systems," *Phys. Rev.*, vol. 46, no. 7, pp. 618–622, Oct. 1934.
- [81] M. J. Frisch, M. Head-Gordon, and J. A. Pople, "A direct MP2 gradient method," *Chem. Phys. Lett.*, vol. 166, no. 3, pp. 275–280, 1990.
- [82] D. Cremer, "Møller-Plesset perturbation theory: from small molecule methods to methods for thousands of atoms," *Wiley Interdiscip. Rev. Comput. Mol. Sci.*, vol. 1, no. 4, pp. 509–530, Jul. 2011.
- [83] M. Kallay, J. Gauss, and P. G. Szalay, "Analytic first derivatives for general coupled-cluster and configuration interaction models," *J. Chem. Phys.*, vol. 119, no. 6, pp. 2991–3004, Aug. 2003.
- [84] R. J. Bartlett and G. D. Purvis, "Many-body perturbation theory, coupled-pair many-

- electron theory, and the importance of quadruple excitations for the correlation problem,” *Int. J. Quantum Chem.*, vol. 14, no. 5, pp. 561–581, Nov. 1978.
- [85] G. D. Purvis and R. J. Bartlett, “A full coupled-cluster singles and doubles model: The inclusion of disconnected triples,” *J. Chem. Phys.*, vol. 76, no. 4, pp. 1910–1918, Feb. 1982.
- [86] J. A. Pople, M. Head-Gordon, and K. Raghavachari, “Quadratic configuration interaction. A general technique for determining electron correlation energies,” *J. Chem. Phys.*, vol. 87, no. 10, pp. 5968–5975, Nov. 1987.
- [87] K. A. Baseden and J. W. Tye, “Introduction to density functional theory: Calculations by hand on the helium atom,” *J. Chem. Educ.*, vol. 91, no. 12, pp. 2116–2123, 2014.
- [88] W. Kohn and L. J. Sham, “Self-consistent equations including exchange and correlation effects,” *Phys. Rev.*, vol. 140, no. 4A, p. A1133, Nov. 1965.
- [89] B. G. Johnson, P. M. W. Gill, and J. A. Pople, “The performance of a family of density functional methods,” *J. Chem. Phys.*, vol. 98, no. 7, pp. 5612–5626, Apr. 1993.
- [90] A. D. Becke, “Density-functional exchange-energy approximation with correct asymptotic behavior,” *Phys. Rev. A*, vol. 38, no. 6, pp. 3098–3100, Sep. 1988.
- [91] A. D. Becke, “Density-functional thermochemistry. III. The role of exact exchange,” *J. Chem. Phys.*, vol. 98, no. 7, pp. 5648–5652, Apr. 1993.
- [92] C. Lee, W. Yang, and R. G. Parr, “Development of the Colle-Salvetti correlation-energy formula into a functional of the electron density,” *Phys. Rev. B*, vol. 37, no. 2, pp. 785–789, Jan. 1988.
- [93] A. Karton, “A computational chemist’s guide to accurate thermochemistry for organic molecules,” *Wiley Interdiscip. Rev. Comput. Mol. Sci.*, vol. 6, no. 3, pp. 292–310, 2016.
- [94] R. A. Friesner, “Ab initio quantum chemistry: Methodology and applications,” *Proceedings of the National Academy of Sciences of the United States of America*, vol. 102, no. 19. National Academy of Sciences, pp. 6648–6653, 10-May-2005.
- [95] J. A. Pople, M. Head-Gordon, D. J. Fox, K. Raghavachari, and L. A. Curtiss, “Gaussian-1 theory: A general procedure for prediction of molecular energies,” *J.*

- Chem. Phys.*, vol. 90, no. 10, pp. 5622–5629, May 1989.
- [96] L. A. Curtiss, K. Raghavachari, G. W. Trucks, and J. A. Pople, “Gaussian-2 theory for molecular energies of first- and second-row compounds,” *J. Chem. Phys.*, vol. 94, no. 11, pp. 7221–7230, 1991.
- [97] L. A. Curtiss, K. Raghavachari, P. C. Redfern, V. Rassolov, and J. A. Pople, “Gaussian-3 (G3) theory for molecules containing first and second-row atoms,” *J. Chem. Phys.*, vol. 109, no. 18, pp. 7764–7776, Nov. 1998.
- [98] L. A. Curtiss, P. C. Redfern, and K. Raghavachari, “Gaussian-4 theory,” *J. Chem. Phys.*, vol. 126, no. 8, p. 084108, Feb. 2007.
- [99] N. J. DeYonker, T. R. Cundari, and A. K. Wilson, “The correlation consistent composite approach (ccCA): An alternative to the Gaussian-n methods,” *J. Chem. Phys.*, vol. 124, no. 11, p. 114104, Mar. 2006.
- [100] N. J. DeYonker *et al.*, “The correlation-consistent composite approach: Application to the G3/99 test set,” *J. Chem. Phys.*, vol. 125, no. 10, 2006.
- [101] J. W. Ochterski, G. A. Petersson, and J. A. Montgomery, “A complete basis set model chemistry. V. Extensions to six or more heavy atoms,” *J. Chem. Phys.*, vol. 104, no. 7, pp. 2598–2619, Feb. 1996.
- [102] J. A. Montgomery, M. J. Frisch, J. W. Ochterski, and G. A. Petersson, “A complete basis set model chemistry. VI. Use of density functional geometries and frequencies,” *J. Chem. Phys.*, vol. 110, no. 6, pp. 2822–2827, Feb. 1999.
- [103] J. A. Montgomery, M. J. Frisch, J. W. Ochterski, and G. A. Petersson, “A complete basis set model chemistry. VII. Use of the minimum population localization method,” *J. Chem. Phys.*, vol. 112, no. 15, pp. 6532–6542, Apr. 2000.
- [104] P. L. Fast, M. L. Sánchez, and D. G. Truhlar, “Multi-coefficient Gaussian-3 method for calculating potential energy surfaces,” *Chem. Phys. Lett.*, vol. 306, no. 5–6, pp. 407–410, Jun. 1999.
- [105] B. J. Lynch and D. G. Truhlar, “Robust and affordable multicoefficient methods for thermochemistry and thermochemical kinetics: The MCCM/3 suite and SAC/3,” *J. Phys. Chem. A*, vol. 107, no. 19, pp. 3898–3906, May 2003.

- [106] L. A. Curtiss, P. C. Redfern, and K. Raghavachari, "Gaussian-4 theory," *J. Chem. Phys.*, vol. 126, no. 8, 2007.
- [107] C. Peng, P. Y. Ayala, H. B. Schlegel, and M. J. Frisch, "Using redundant internal coordinates to optimize equilibrium geometries and transition states," *J. Comput. Chem.*, vol. 17, no. 1, pp. 49–56, Jan. 1996.
- [108] R. F. Stewart, "Small Gaussian Expansions of Slater-Type Orbitals," *J. Chem. Phys.*, vol. 52, no. 1, pp. 425–431, Jan. 1970.
- [109] V. A. Rassolov, M. A. Ratner, J. A. Pople, P. C. Redfern, and L. A. Curtiss, "6-31G* basis set for third-row atoms," *J. Comput. Chem.*, vol. 22, no. 9, pp. 976–984, Jul. 2001.
- [110] R. Ditchfield, W. J. Hehre, and J. A. Pople, "Self-consistent molecular-orbital methods. IX. An extended gaussian-type basis for molecular-orbital studies of organic molecules," *J. Chem. Phys.*, vol. 54, no. 2, pp. 720–723, Jan. 1971.
- [111] A. V. Marenich, C. J. Cramer, and D. G. Truhlar, "Universal solvation model based on solute electron density and on a continuum model of the solvent defined by the bulk dielectric constant and atomic surface tensions," *J. Phys. Chem. B*, vol. 113, no. 18, pp. 6378–6396, May 2009.
- [112] A. V. Marenich, C. J. Cramer, and D. G. Truhlar, "Universal solvation model based on the generalized born approximation with asymmetric descreening," *J. Chem. Theory Comput.*, vol. 5, no. 9, pp. 2447–2464, Sep. 2009.
- [113] M. J. Frisch *et al.*, "Gaussian 16, Revision B.01," p. Gaussian 16, Revision B.01, 2016.
- [114] R. . K. T. and M. J. Dennington, "Gauss View, Version 5," *Semichem Inc.*, 2009.
- [115] C. Gonzalez and H. Bernhard Schlegel, "An improved algorithm for reaction path following," *J. Chem. Phys.*, vol. 90, no. 4, pp. 2154–2161, Feb. 1989.
- [116] L. A. Curtiss, P. C. Redfern, K. Raghavachari, V. Rassolov, and J. A. Pople, "Gaussian-3 theory using reduced Møller-Plesset order," *J. Chem. Phys.*, vol. 110, no. 10, pp. 4703–4709, Mar. 1999.
- [117] A. G. Baboul, L. A. Curtiss, P. C. Redfern, and K. Raghavachari, "Gaussian-3 theory using density functional geometries and zero-point energies," *J. Chem. Phys.*, vol. 110,

- no. 16, pp. 7650–7657, Apr. 1999.
- [118] A. D. Becke, “Density-functional thermochemistry. III. The role of exact exchange,” *J. Chem. Phys.*, vol. 98, no. 7, pp. 5648–5652, Apr. 1993.
- [119] D. R. Lide, *CRC handbook of chemistry and physics*, 90th ed. Boca Raton, FL: CRC Press/Taylor and Francis, 2010.
- [120] P. Król and J. Wojturska, “Kinetic study on the reaction of 2,4- and 2,6-tolylene diisocyanate with 1-butanol in the presence of styrene, as a model reaction for the process that yields interpenetrating polyurethane-polyester networks,” *J. Appl. Polym. Sci.*, vol. 88, no. 2, pp. 327–336, Apr. 2003.
- [121] C. O. C. López, Z. Fejes, and B. Viskolcz, “Microreactor assisted method for studying isocyanate–alcohol reaction kinetics,” *J. Flow Chem.*, vol. 9, no. 3, pp. 199–204, Sep. 2019.
- [122] G. Raspoet, M. T. Nguyen, M. McGarraghy, and A. F. Hegarty, “The alcoholysis reaction of isocyanates giving urethanes: Evidence for a multimolecular mechanism,” *J. Org. Chem.*, vol. 63, no. 20, pp. 6878–6885, Oct. 1998.
- [123] M. Çoban and F. A. S. Konuklar, “A computational study on the mechanism and the kinetics of urethane formation,” *Comput. Theor. Chem.*, vol. 963, no. 1, pp. 168–175, 2011.
- [124] F. Kössl, M. Lisaj, V. Kozich, K. Heyne, and O. Kühn, “Monitoring the alcoholysis of isocyanates with infrared spectroscopy,” *Chem. Phys. Lett.*, vol. 621, no. 621, pp. 41–45, Feb. 2015.
- [125] X. Wang *et al.*, “DFT Study of the Proton Transfer in the Urethane Formation between 2,4-Diisocyanatotoluene and Methanol,” *Bull. Chem. Soc. Jpn.*, vol. 86, no. 2, pp. 255–265, Feb. 2013.
- [126] K. SOMEKAWA, M. MITSUSHIO, and T. UEDA, “Molecular Simulation of Potential Energies, Steric Changes and Substituent Effects in Urethane Formation Reactions from Isocyanates,” *J. Comput. Chem. Japan*, vol. 15, no. 2, pp. 32–40, 2016.
- [127] I. Akiyama, M. Ogawa, K. Takase, T. Takamuku, T. Yamaguchi, and N. Ohtori, “Liquid structure of 1-propanol by molecular dynamics simulations and X-ray scattering,” *J. Solution Chem.*, vol. 33, no. 6–7, pp. 797–809, Jun. 2004.

- [128] A. Baev, *Specific intermolecular interactions of nitrogenated and bioorganic compounds. Heidelberg, Germany: Springer, 2013.* *Specific intermolecular interactions of nitrogenated and bioorganic compounds.* Heidelberg, Germany: Springer, 2013.
- [129] V. Majer, V. Svoboda, and H. Kehiaian, “Enthalpies of vaporization of organic compounds: a critical review and data compilation,” 1985.
- [130] V. Lenzi, P. J. Driest, D. J. Dijkstra, M. M. D. Ramos, and L. S. A. Marques, “GAFF-IC: realistic viscosities for isocyanate molecules with a GAFF-based force field,” *Mol. Simul.*, vol. 45, no. 3, pp. 207–214, Feb. 2019.
- [131] V. Lenzi, P. J. Driest, D. J. Dijkstra, M. M. D. Ramos, and L. S. A. Marques, “Investigation on the intermolecular interactions in aliphatic isocyanurate liquids: revealing the importance of dispersion,” *J. Mol. Liq.*, vol. 280, pp. 25–33, Apr. 2019.
- [132] A. Al Nabulsi, D. Cozzula, T. Hagen, W. Leitner, and T. E. Müller, “Isocyanurate formation during rigid polyurethane foam assembly: A mechanistic study based on: In situ IR and NMR spectroscopy,” *Polym. Chem.*, vol. 9, no. 39, pp. 4891–4899, Oct. 2018.
- [133] T. Stern, “Hierarchical fractal-structured allophanate-derived network formation in bulk polyurethane synthesis,” *Polym. Adv. Technol.*, vol. 29, no. 2, pp. 746–757, Feb. 2018.
- [134] E. Delebecq, J. P. Pascault, B. Boutevin, and F. Ganachaud, “On the versatility of urethane/urea bonds: Reversibility, blocked isocyanate, and non-isocyanate polyurethane,” *Chemical Reviews*, vol. 113, no. 1. American Chemical Society, pp. 80–118, 09-Jan-2013.
- [135] K. Pietrzak, M. Kirpluks, U. Cabulis, and J. Ryszkowska, “Effect of the addition of tall oil-based polyols on the thermal and mechanical properties of ureaurethane elastomers,” *Polym. Degrad. Stab.*, vol. 108, pp. 201–211, Oct. 2014.
- [136] A. Eceiza *et al.*, “Structure-property relationships of thermoplastic polyurethane elastomers based on polycarbonate diols,” *J. Appl. Polym. Sci.*, vol. 108, no. 5, pp. 3092–3103, Jun. 2008.
- [137] M. A. P. G. Christian M. Lehmann, “Process for making low density flexible polyisocyanurate-polyurethane foams,” *Elastomers Plast.*, vol. 14, Jan. 1990.

- [138] Monument Chemical, “Terms and Formulas Used in Urethane Polymer Preparations,” 2010.
- [139] M. Ashby, “Materials selection in mechanical design: Fourth edition,” *Mater. Sel. Mech. Des. Fourth Ed.*, vol. 9780080952, pp. 1–646, 2010.